Simulation of Ultrasound Computed Tomography in Diffraction Mode

by

Tejaswi Thotakura, B. Tech.,
J B Institute of Engineering and Technology,2011

A thesis submitted to the Faculty of Graduate and Postdoctoral Affairs in partial fulfillment of the requirements for the degree of

Masters of Applied Science in Biomedical Engineering

Ottawa-Carleton Institute for Biomedical Engineering
Department of Systems and Computer Engineering
Carleton University
Ottawa, Ontario

Abstract

Ultrasound computed tomography (USCT) aims at safe and fast high resolution imaging but due to its complexity and time consuming reconstruction procedures this imaging modality is not commercial in use. One can imagine USCT as an imaging procedure where X-rays source in a computed tomography scanner are replaced by ultrasound source, but in practice the straight ray tomographic imaging principle cannot be directly applied because ultrasound does not travel in a simple straight line alone. It undergoes diffraction due to relatively large wavelengths associated with typical ultrasound sources. USCT which considers diffraction property of tissues is said to be working in diffraction mode. In this research, we analyze Ultrasound computed tomography in diffraction mode. The wave equation is theoretically and numerically solved with Helmholtz equation using Green's function under consideration of various approximations to linearize the integral representation while considering the diffraction of wave is due to scattering terms as a function of compressibility and velocity. The received field found by solving wave equation was simulated. We also propose a new approach for reconstructing the parameters of interest. These simulation results indicate that proposed method can yield images with higher image resolution with a better computation time compared to other existing models.

Acknowledgement

First of all, I would like to sincerely thank my supervisor Dr. Chris Joslin (School of Information Technology, Carleton University), for his tremendous support and guidance during the course of this research. His valuable suggestions have consistently helped me in this thesis work, and have greatly contributed to the quality of the thesis. I would like to acknowledge Dr. WonSook Lee (School of Information Technology and Engineering, University of Ottawa) for her academic support. I would also like to thank my institution (Carleton University) which has been a great platform for fulfilling my dream of higher education.

Finally, I would like to thank my parents and friends for their love and support.

Table of Contents

List of Tables

List of figures

List of Abbreviations:

CT- Computed Tomography

CIHI- Canadian Institute for Health Information

EQ-Equation

FOV- Field of View

FT- Fourier Transform

LSI- Linear Shift Invariant

MRI- Magnetic Resonance Imaging

NUFT- Non-Uniform Fourier Transform

NUFFT- Non-Uniform Fast Fourier Transform

PET- Positron Emission Tomography

SPECT- Single Photon Emission Computed Tomography

SOS- Speed of Sound

3D- Three Dimensional

2D- Two Dimensional

TOF- Time Of Flight

T/R- Transmitter/Receiver

TR-Tikhonov Regularization

USCT- Ultrasound Computed Tomography

1 Chapter: Introduction

1.1 Medical Imaging

The desire to analyze the internal body structure in detail without causing any harm to the body is the key foundation for the invention of any imaging modality. The basic principle behind medical imaging is targeting a subject with some kind of energy and collecting the response through receivers and analyzing the collected data to form images of the subject of interest. These images (obtained from the data) are used to visualize the internal body and analyze (diagnose) the diseases. There are currently many different kinds of medical imaging modalities which are either categorized as invasive or non-invasive. Few examples of non-invasive imaging modalities are Projection Radiography, Magnetic Resonance Imaging (MRI), Computed Tomography (CT), Nuclear medicine imaging and Ultrasound Imaging.

The concept of medical imaging was initiated with invention of X-rays by Wilhelm Conrad Röntgen in 1895. Medical imaging was a breakthrough invention alongside the discovery of anesthesia and antibiotics in the medical history because it entirely changed the way doctors could diagnose, treat, or even think about a medical condition. This imaging enabled doctors to treat internal body parts without surgically opening it or blood loss, or any other bodily harm. In 1800 century, the doctors had to cut open to see or analyze the medical problem to treat it. For example, consider in the case of any heart issue a physician has to cut open the body to have a better view of it, irrespective of state and severity of the problem. With the invention of medical imaging the diagnosis of heart disease became very convenient and the exact problem can be readily understood without actually cutting open the body and also treated non-invasively

without the risk of infection. Hence saving a lot of time, money and any further infections or risk associated with open cuts. Medical imaging was beneficial in terms of cost, time and health. Nowadays many diseases are analyzed and cross checked with medical imaging. It has a wide area of application from viewing a simple bone fracture to analyzing the functioning of brain or visualizes a cancer tumor and determines how well a cancer drug would work. These analysis reports generated with help of devices such as CT, MRI, Ultrasound imaging also reduce guesswork. Medical imaging devices can also be used as regulating and monitoring devices. Though most of the imaging modalities are for diagnosis, but some also serve therapeutic use like the Cavitron Ultrasonic Surgical Aspirator (or CUSA).

1.2 Motivation

Ever since the invention of medical imaging technology, it has been evolving, bringing more comfort and clinical advantages in various medical application such as cancer drug delivery systems, cardiac imaging system and so on. According to Global Medical Imaging Market Report, 2013 Edition, the number of medical imaging device market has grown exceptionally over the past few years worldwide, owing to rise of an aging population pool, emergence of new diseases, expanding of the middle class population, improvements in functional imaging, healthcare reforms and increased number in emerging markets. These industries always compete with creative and patient-friendly solutions that are convenient, safe and easy to use.

In the Global Medical Imaging Market Report, 2013 Edition,[64] it is estimated that Global market for medical imaging devices is around USD $30.2 billion and is anticipated it to be USD $32.3 billion by 2014, which may further exceed to USD $49

billion by 2020. In this global scale North America stands on the top with a major portion of the shares, followed by Europe, Japan and China. CT, MRI, Positron Emission Tomography (PET), Ultrasound and X-Ray are the most popular medical imaging devices and make largest segment of market share globally. The other trend devices are combined systems such as PET-MRI or PET-CT, etc. According to data released by Canadian Institute for Health Information (CIHI) [63] in 2013; as of January 1st, 2012, there were 308 MRI scanners and 510 CT scanners operational in Canada. This represents an increase of 15 MRI and 8 CT scanners over the previous year and an increase of 151 MRI and 169 CT scanners since 2004.

As the number of medical imaging devices increases, so as the medical examinations performed increases. According CIHI, [63] 1.7 million magnetic resonance imaging (MRI) exams and 4.4 million computed tomography (CT) exams were performed in Canada in 2011–2012. As compared during the past 10 years, this was a tremendous increase. This statistics reveal the importance of medical imaging device and its influence on global economic market. On the other note, the increase in these medical exams shows the dependency of practitioners on medical imaging. These statistics reveals the importance is medical imaging devices.

Although all medical imaging devices generate images, few imaging techniques are risk oriented due to radiation exposure like projection radiography, CT, fluoroscopy etc. and while few are expensive too. During an X-ray procedure, an individual is exposed to a flash of radiation that produces a two dimensional image of the body on the film. CT scanner has a rotating x-ray source that flashes x-rays throughout the body to produce three dimensional images. This scan gives sharper images but exposes body to

more radiation. A single CT scan gives a patient as much radiation as 50 to 800 chest X-rays. During nuclear medicine imaging, such as Positron Emission Tomography (PET) scan, a radiotracer is ingested into the body and detector captures its activities and forms an image. Nuclear medicine procedure exposes a patient to radiation as much as 10 to 2,000 chest X-rays. The table below gives an overview of the average effective doses from X-rays, CT scans and Nuclear medicine on various body parts [54].

Table 1.1 Average Effective Dose (in mSv) for Various Procedures

Examination	X-ray	CT scan	Nuclear medicine
Head	-	2	7-14
Neck	-	3	2-5
Chest	0.1	7	0.2 - 40.7 (cardiac stress test)
Abdomen	0.7	8	0.4-7.8
Spine	1.5	6	-
Pelvic	0.7	6	-

The risk of developing cancer from a single scan is very small but multiple exposures to radiation may increase the risk. The earth's atmosphere has radiation exposure of about 3 millisieverts (mSv) per year which comes from natural sources and hasn't changed since 1980, but the accumulative total radiation exposure that comes from medical imaging devices doubles every year and the proportion of total radiation exposure is on an average of 20 mSv per year, with a maximum of 50 mSv in any single year. In Canada alone, there are 4.4 million computed tomography (CT) exams were performed in 2011–2012

[63], which shows the rate of radiation exposure. On the other hand, devices such as MRI do not have radiation exposure but have lengthy time consuming procedure that lasts approximately between 15 to 90 minutes (depending on the area to be scanned) and a long wait time too.

Overall, every medical imaging device has its own advantages and specific functionality and its own drawbacks. In this modern era, improved technology and spread of knowledge have made the general public smarter and more health conscious. Hence, when it comes to health care, they would rather prefer to choose an easy and safe medical procedure and of course, economical too. Hence, the general public tends to opt for a safe and economical trending medical imaging technique wherever applicable rather than any other technique. This builds the main motivation behind our research i.e. to improvise a safe medical imaging technique which is easy to perform and economical compared with existing medical examination. Ultrasound Computed tomography (USCT) is one which imaging modality which aims at safe i.e. radiation free imaging modality. USCT is a hybrid technique which combines CT techniques with ultrasound. Tomography is derived from Greek words ‘tomos’ meaning "slice or section" and graphein "to write". So usually tomography refers to take 2D images in slices and reconstructing back into 3D images. USCT as the name implies uses ultrasound for sliced images and then reconstructs back into detailed image using computer software tools for better diagnosis. In short, USCT is an imaging procedure where X-rays in a CT scanner are replaced by ultrasound wave which aims at safer and high resolution imaging. Ultrasound waves in clinical use are known to be less hazardous to human body when operating under ‘safe zone’ conditions [10]. It is known that sound waves of very high frequencies can easily and harmlessly

penetrate into human flesh at different depths depending on the different frequency. This formulates the basic principle behind this imaging modality. When sound waves are targeted on the body through an ultrasound transducer, they enter the body and confront different materials such as the blood, bone, tissues and internal organs. These materials with various acoustic impedance cause waves to reflect back to the transducer differently. Since the waves reflect back differently at different timings, a technician or the physician can identify the type of material by the nature of the reflection or diffraction or transmission. USCT has a number of advantages which includes non-invasiveness, widespread availability, convenient, short examination times and lack of radiation exposure. USCT is more convenient than conventional Ultrasound imaging because it is automated; hence the output is not operator dependent. It also eliminates the superimposition problem in conventional ultrasound imaging, as it provides multidimensional images of the body giving a better view of organ lying beneath the bones or cavities.

1.3 Problem Statement

Ultrasound imaging is a considerably safe imaging procedure with minimal known effect and economical compared to CT or MRI examination cost. It is quick and convenient, compared to techniques such as CT or MRI scans. USCT is a hybrid device which helps in improving the field of view and eliminates operator dependent artefacts as well. But the major application of ultrasound computed tomography is for tumor detection in very soft tissues like breast, prostate, etc. Majority of the research on USCT is devoted for imaging small and soft tissue organs and application of USCT on larger areas or whole body scanning is still a challenge.

Based on the research, the problem is USCT considers ultrasound wave as a ray assuming it travels in a straight line during propagation and embeds ray statistics. While considering smaller organ with uniform tissue such as breast, prostate, etc. the above assumptions are valid because ultrasound travels in straight line in homogeneous medium of smaller diameter. In reality, while considering the whole body scanning which is non-homogenous medium this assumption fails because ultrasound is a kind of sound wave, which has properties of sound i.e. it does not travel in straight line unlike rays, but it can scatter (diffract) too. Especially, when size of objects is much smaller than the wavelength of ultrasound, ray statistics cannot be applied. Applying ray statistics for ultrasound wave loses the essential components or details of the images. Therefore compromising on the resolution of the image and involves complex computational and time consuming methods.

Ultrasound computed tomography model in specific is slightly different and conventional tomography principles cannot be applied directly because it undergoes multiple deflections and diffraction too. Also propagation speed of ultrasound is so low such that delay in propagation times can also be measured and various methods have been suggested to deal with these refractive problems [5, 30, 31] but still under clinical trials.

Hence in case of ultrasound study, diffraction theory is necessary. If an USCT system considers diffraction mode imaging i.e. if it considers the diffraction property of ultrasound, then the system may produce quality images with good resolution because ultrasound wave diffracts when it encounters objects that are smaller than its wavelength. The goal of our thesis is to develop an ultrasound computed tomography system which

considers diffraction property of ultrasound waves such that the details are conserved which adds up to high resolution images by reducing the computation complexity and improving time consuming reconstruction methods.

1.4 Proposed Method

When ultrasound penetrates through an inhomogeneous medium, it undergoes diffraction and creating a scattered pressure field in the output. The characteristic of the scattered field reveals the tissue property. This scattered field forms the base of the ultrasound diffraction tomography. An USCT system which considers diffractive property of US is said to be working in Diffraction mode. USCT in diffraction mode is almost similar to reflection tomography where instead of summing all the received signals, each one is separately recorded and reconstructed taking the Fourier transform of each received signal with respect to time.

USCT in Diffraction mode uses an alternate approach known as inverse scattering problem for reconstructing the parameters of interest. The direct scattering theory and inverse scattering theory fall under scattering problem theory. The direct scattering theory is to determine the relation between input and output waves based on the known details about the scattering target. The inverse scattering theory is to determine properties of the target based on the computed input-output pairs. Tomographic reconstruction in diffraction mode uses inverse scattering approach also known as forward scattering problem. Commonly scattering problem is solved with Lippmann-Schwinger or Integral equation using Green's function.

Iwata and Nagata [2] were first to bring in the idea of ultrasonic tomography where they calculated refractive index distribution of object of interest using the Born

and Rytov's approximation. Later, Mueller et al. [3] and Stenger et al. [4] investigated on this method through various reconstruction algorithms. Many computer simulations testing these methods have met success but the not clinical applied till present due to its high complexity and computational time.

USCT working in diffraction mode can be explained using a model in Figure 1. In this, let us assume the system works on single transducer (T/R) and the object of interest are placed at a distance from the transducer. A transducer usually acts as both transmitter and receiver. When the transducer is excited by voltage, the object is insonified by ultrasound transducer forming a wide cone shaped beam. In the cone-beam case, circular-arc wave fronts are produced, while, in the plane-wave case, the wave fronts consist of parallel straight lines.

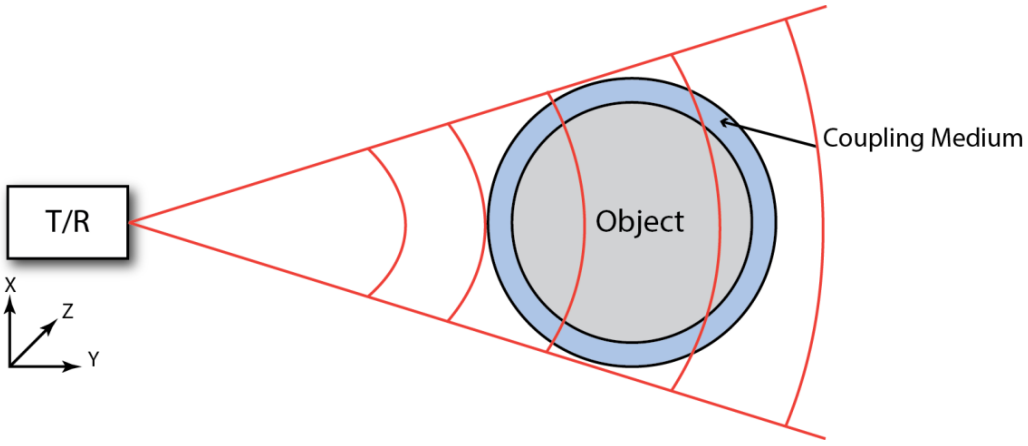

Figure 1: USCT in Diffraction Mode

When Ultrasound penetrates through an inhomogeneous medium, it undergoes diffraction and creating a scattered field in the output. The characteristic of the scattered field reveals the tissue property. This scattered field forms the base of the ultrasound diffraction tomography. The essential components for supporting the ultrasound diffraction tomography are:

- Firstly, a mathematical model describing the tissue-sound interaction and parameters of interest. We have solved the wave equation for non-homogeneous medium, considering change in compressibility and density of the tissue which accounts for the scattering term. This equation was solved using Born's approximation. A paper on this mathematical derivation was published for The Journal of Macro Trends in Health and medicine, Monaco, 2014 [Author related Publications 1]
- Secondly, a reconstruction procedure to deduce the parameter of interest from the measured solutions. The above inverse scattering problem which is established based on wave theory can be ill posed equation. Reconstruction of the image from the above formulated equation can be very time consuming because it has no proper converging point.
- This ill posed problem can be solved into well posed by introducing a regularization term. Regularization is a process of proposing an additional term to an ill-posed problem to prevent it from over fitting. One such is the Tikhonov regularization which is a popular approach to solve discrete ill-posed problems. But its applicability on ultrasound diffraction problem was tested using a computer simulation where the scattering term can be estimated using Tikhonov regularization using the equation below where α is the regularization parameter.

$$O=\min\| P_s-MO\|^2 + \alpha\|L_1\|^2$$

O was updated with iteration by Tikhonov regularization with l1 regularization norm. Introduction of this regularization term during non-uniform fast Fourier transform reconstruction yields images with high resolution. It also reduces the

complexity and decreases the reconstruction time. A paper on regularization in ultrasound computed tomography was conferred for The Global Academic Network International Conferences, Ottawa, 2014 and is due for publishing in late 2014 [Author related publication 2].

1.5 Organization of Thesis

The first part of the thesis, which is chapter 2, gives an overview about Ultrasound Computed tomography and few essential related theories like Ultrasound field-medium interactions such as reflection, transmission, diffraction, etc. followed by few fundamental concepts which help in better understanding of the research. This chapter also introduces to ultrasound computed tomography principle and its importance and the state of art of existing ultrasound computed tomography modes and architectures. Chapter 3 introduces about ultrasound computed tomography in diffraction mode and its principle, followed by wave equation derivation to theoretically support diffraction theory. The next following chapter 4 involves different reconstruction procedures and importance of regularization in reconstruction. The theoretical and numerical method is proved with a computer simulation. Chapter 5 deals with simulations and the obtained results. The research thesis concludes with discussion and scope of future work.

2 Chapter: Literature Review

2.1 State of Art:

The history of ultrasound dates back in 1940's, when Dr. F. A. Firestone [62] at the University of Michigan saw images of bones with a device named "supersonic reflectoscope" patented in 1942. This device was used to detect flaws in metals, by the reflections of high-frequency ultrasound sound waves radiated by quartz crystal. Dr. F. A. Firestone noticed that an ultrasound wave has the ability to penetrate into the human body without the accompanying hazards of X-radiation.

This soon attracted medical researchers and not many years later; medical researchers began to realize that the principle might be applied to a new kind of x-ray-less medical devices for studying the internal structures of the human body. In the same year, Firestone's first explorations of low energy ultrasound as a diagnostic tool were being carried out by K.T. Dussik. However, Dussik used the new tool like an x-ray, passing sound through the patient to get the kind of shadow picture on film. Moreover, he worked on human head, so the high absorption of the skull virtually defeated the transmission technique. Doctor Karl Theodore Dussik of Austria, in 1942, had published the first paper on medical ultrasonic. He extended the investigation of ultrasound transmission into different larger parts of the human body like the brain [2] [3]. It was the echo-location technique of Firestone that has gained popularity. The practical implementation of ultrasound was performed in 1950 by Professor Ian Donald of Scotland. Rapid expansion of ultrasound imaging system began in early 1970s, with the advent of two-dimensional real-time ultrasonic scanners. Many other contribution towards ultrasound imaging device to be noted were the appearance of phased array

systems in early 1980s, color flowing-imaging systems in the mid 1980's and three-dimensional imaging systems in the 1990's. The progress in the field of ultrasound study has seen a considerable rise in the past couple of years, enhancing the accuracy of diagnostic inference and reducing variability in drawing conclusions and improving the full Field-of-view (FOV).

The concept of tomography dates back to the early 1900s where an Italian radiologist Alessandro Vallebona proposed an approach to represent a single slice of the body on the radiographic film. And in later phase computer was invented and then came into play was computed tomography scanner (CT scanner). CT-scanner was one of the classic inventions to image the body and visualize the images of body in all the three dimensions. James F Greenleaf was the first to bring about the idea of possibility of using ultrasound instead of X-rays in a computed tomography technique. He published his paper on Ultrasound computed tomography in the year 1974 [5]. Ultrasound tomography is a technique that uses ultrasound waves for obtaining sliced projection images of the object of interest and then reconstructs back into detailed image. Over the past few decades several researchers have proven the capabilities of ultrasound tomography to reconstruct the acoustic parameters like acoustic speed and attenuation. Initial works have mapped attenuation coefficient and speed of sounds to reconstruct the scanned images.
Some of the striking advancement in the ultrasound computed tomography (USCT) is its capability of simultaneous recording of reproducible attenuation and speed of sound volumes, reflection, high image quality, and fast data acquisition. Few researchers focused on improving acoustic radiation force penetration and produce stronger shear waves so it could penetrate in deep tissues where few focus on the role of ultrasound

image analysis on certain specific organs of interest. [7][8] These advancements also gave a new directions and approach to ultrasound for a better image quality.

All together based on the propagation of ultrasound in the object of interest (medium) these methods can categorizes USCT under three modes;

1.) Transmission mode
2.) Reflection mode
3.) Diffraction mode

James F. Greenleaf [5] was the first who has come up with the idea of ultrasound transmission tomography. Greenleaf et al. have worked on reconstruction of the acoustic attenuation coefficient to map the image. Several other researchers later explored mapping with the attenuation coefficient or the speed of sound or any other means for reconstruction and also tried to test the clinical applicability. In general a projection of image of the object of interest with USCT in transmission mode can be made by either comparing the amplitude of the pulses which is used to reconstruct the acoustic attenuation or using time-of-flight (ToF) measurement which then used to reconstruct speed of sound (SoS).

Ultrasound computed tomography (USCT) in reflection mode works based on measurements of line integrals of the reflectivity of object of interest. In 1970 and 1980's, Johnson et al., Norton et al [30] and Kim et al [31] have contributed tremendously for USCT in reflection mode. But till date the research still continues to reconstruct a quantitative cross- sectional image from reflection data to improve spatial resolution.

There is not much research going on diffraction tomography and all the literature reviews are very vague or concentrated more for geographical approach or used for constructional problems. But USCT diffraction tomography as discussed earlier uses an

alternate approach known as inverse scattering problem for reconstructing the parameters of interest. An USCT system which considers diffractive property of US is said to be working in Diffraction mode. USCT in diffraction mode is almost similar to reflection tomography where instead of summing all the received signals, each one is separately recorded and reconstructed taking the Fourier transform of each received signal with respect to time.

M. Ashfaq and H. Ermert [46] have tried to embed a module of ultrasound tomography in transmission mode to the standard ultrasound system set up .This transmission mode also allows spatially resolved tomographic reconstruction of parameters like acoustic speed and acoustic attenuation. This system used two linear array transducer as shown in Figure 2 that rotate around the object which would simultaneously collect and analyze data from the object in multiple direction.

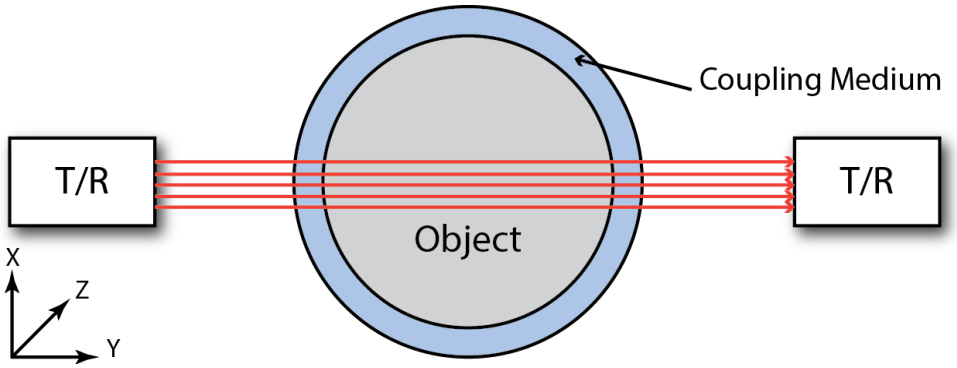

Figure 2 : Ultrasound Tomography in Transmission Mode Using Two Linear Array of Transducer

It was designed to extend the functionality of the ultrasound system as well as improve the spatial resolution and reconstruction capability. But they haven't explained the cause the cause of the attenuation and frequency dependence of attenuation reconstruction. As

technologies improve over the years, so has the ultrasound device but the basic concept always remains the same.

One more recent latest advancements in three dimensional diagnostic imaging technology are known as “multimodal ultrasonic tomography” (MUT), [11] this method has drawn the attention of the researchers for its capability of detection of breast cancer without the ionizing radiation or the compression. There is a considerable difference in the approach of MUT compared to conventional B-mode ultrasound imaging device. MUT constructs tomographic images in transmission mode using the acoustic attributes of refractivity, frequency-dependent attenuation and dispersion at each tissue voxel. The B-mode ultrasound and the “whole breast ultrasound imaging” systems generate a sequence of B-mode images automatically. Thus, the information content of MUT images is distinct from the echo-mode ultrasound currently in use and the recently introduced “whole-breast ultrasound” images. Proper analysis of waveform changes in the received pulse, relative to water-through propagation enables the MUT technology to generate multiple images for each coronal slice. Different tissues have different and distinctive combinations of acoustic refractivity, attenuation and dispersion. Thus, MUT could help characterize tissues, and differentiate lesions [11].

The ultrasound computed tomography research was mostly devoted for tumors detection in soft tissues like breast, prostate, etc. Breast imaging with ultrasound took a fast pace in research and development during past 10 years because it does not involve a painful compression of the breast or radiation. This kind of breast imaging with ultrasound was used where the effectiveness of mammography may be limited.

Automated breast imaging is an approach to minimize human error, which is a common problem with conventional ultrasound [47]. In this system transducers are attached to an automated handle operated by a computer which then automatically scans a woman's breast capturing multiple ultrasound images and displaying them in 3D for review by a physician. GE health care developed this system and was approved by FDA in 2012. "Automated Breast Ultrasound (ABUS™)" system is specifically for breast cancer screening in women with dense breast tissue. The SonoCine "Automated Whole Breast Ultrasound System (AWBUS)" was another automated breast ultrasound system invented and created by SonoCine Inc. a privately owned research, development and manufacturing company with focus on early breast cancer detection. This system is exclusively for providing radiologists with a methodical, adjunctive examination for early detection of mammographically occult breast cancer in women with dense-breast tissue. This system was reported as high cancer detection performance with results of number of vital system characteristics. Together with separating the image data acquisition, maximizing lesion visualization, automating and computer-controlling the screening of the entire breast using dynamic software, from the radiologist's point of view. And unlike MRI and MBI, requires neither contrast agent, nor a radioactive tracer. In February 19, 2014 Royal Philips partnered with SonoCine Inc., a US research, development and manufacturing company to provide automated whole breast ultrasound (AWBUS) image for the Philips EPIQ and iU22 ultrasound system.

Traditional automated ultrasound system is used only for breast imaging which works on analyzing the returning reflected echoes in the direction of the transducer. Such USCT systems captures reflection echoes from all directions around breast and collects

transmitted signals in different projection angles coming through the breast. One such very recent advancement was “SoftVue” by Delphinus Medical Technologies for the diagnosis for breast but is not intended for use as a replacement for screening mammography [48] [49]. This system gas received FDA clearance in April, 2014. The transducer are placed as an array of ring shaped transducers architecture which incorporates over 2000 transducer elements within a uniform ring configuration that studies multi-parameter sound characteristics like reflection, sound speed, echo and attenuation. The SoftVue imaging table has a small groove like structure which has transduces placed as ring shaped architecture (Figure 3) that can move up and down from chest to nipple covering the entire breast

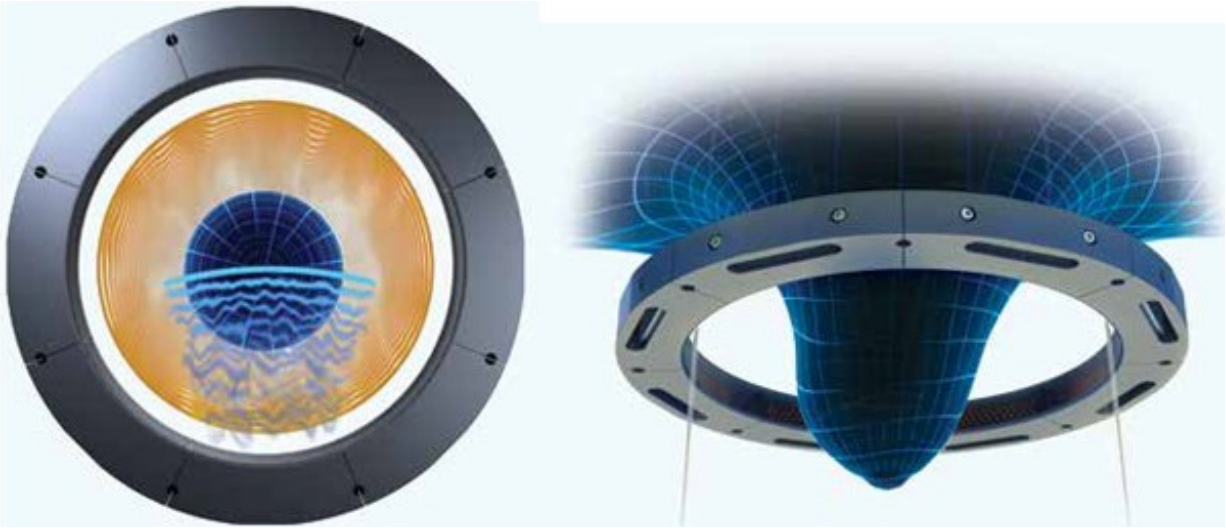

Figure 3: Transducer Arrangement and Image acquisition process [49]

Patient is asked to lie down on the SoftVue imaging table (Figure 4) such that the breast to be imaged is inserted in a small groove filled with water. The water acts as a coupling medium. These transducer elements transmits ultrasound signals into the object to be imaged (i.e. Breast) through the coupling medium, in a sequenced 360° circular array. The signals are collected and stored in a circumferential, tomographic series analyzed by

proprietary algorithms, providing volumetric measurements. These measurement using properties like Sound speed and attenuation are essential in providing breast tissue characterization for analyzing tissue stiffness and density. Therefore, if forms a great platform for analyzing the risk of breast cancer. But this system has not taken curved ray tomography in account.

Figure 4: SoftVue Ultrasound Computed Tomography for Breast Imaging [49]

USCT in 3D domain was successfully implemented and ready for clinical trials. Image quality and resolution in a three dimensional view always in creates a room for future progress. 3D Ultrasound computer tomography (3D-USCT) is used as a device method aimed at early diagnosis of breast cancer. The 3D-USCT has the potential to produce images of resolution well below a millimeter and has high signal to noise ratio. This method is universally accepted and is being used for 3D analysis of sufficient small bodies. For further applicability of the 3D-USCT; the reconstruction time for a high-resolution volume is desired to be less than an hour [41]. Ruiter et al. implemented a prototype of that can acquire breast images in four minutes [42]. During the application

of 3D-USCT for the diagnosis of breast cancer, due to the 3D imaging of the unreformed breast in a prone position, the images from the 3D-USCT device can be registered to MRI volumes easily. This would help in obtaining useful information about the tissue properties. Hence this combination could support the early breast cancer diagnosis.

Ultrasound can be coupled with other sources like magnetic induction provided with good contrast provided by tissue electrical properties for biological imaging. This kind of imaging known as Magneto acoustic tomography with magnetic induction (MAT-MI) [6] .This is a technique to reconstruct the conductivity distribution in biological tissue based on current density at ultrasound imaging resolution. LOUIS-3DM [10] is a novel system developed for preclinical research which combined multi wavelength optoacoustic and laser ultrasound tomography's for in vivo high resolution whole body imaging of small animal models. This system advances to 3D angiography, biological distribution of optoacoustic contrast agents and cancer research. Ultrasound-modulated bioluminescence tomography is a hybrid imaging method for reconstruction the source density in bioluminescence tomography. Their approach is based on the solution to a hybrid inverse source problem for the diffusion equation [50].

Due to technological constraints and lack of availability of super computer it lead to downfall of research on ultrasound computed tomography in 1990's but it took a leap from 2005 onwards due to tremendous contribution from physicist and technologist by inventions of faster reconstruction methods or by improvement of nanotechnology or other complex related programming works. Yet considerable amount of work is being put in for this ultrasound computed tomography system (USCT) development but the majority of USCT system research concentrates on soft tissue imaging and did not

explain much about whole body imaging. This could be possible because of assumption of ultrasound propagation in straight line. Ultrasound propagation in soft tissue is much considerably straight without diffraction, than in any other areas of body. Also ultrasound tomography imaging involves complex and high computation time for reconstruction. Before going further on USCT principles and its working, it better to have a quick overview on USCT related background and theory.

2.2 Related Background

Embracing the basic properties of the ultrasound wave and its interaction with tissues is very essential for better understanding and analyzing of USCT's application and principles. Ultrasound waves are a kind of sound waves which has a frequency that is higher than what the human ear can hear i.e. 20,000 Hz. Ultrasound generally cannot distinguish objects that are smaller than its wavelength. Therefore ultrasound waves with higher frequency produce better resolution than with the lower frequency ultrasound waves. Ultrasound waves have same properties such as a normal sound wave. A one dimensional sound wave equation for pressure *p* moving in a direction, for example assume *z* direction, at instant time *t* with speed *c* is denoted as [60]:

$$\frac{\partial^2 p}{\partial z^2} = \frac{1}{c^2}\frac{\partial^2 p}{\partial t^2} \qquad \textit{(eq2.0)}$$

one of the solutions that satisfy the one dimensional wave equation above is the sinusoidal function;

$$p(z, t) = \cos \kappa(z - ct) \qquad \textit{(eq 2.1)}$$

when solved with respect to function '*t*' holding '*z*' fixed, we analyze that pressure, around a fixed particle varies sinusoidally with a radial frequency $\omega = \kappa c$. This gives a cyclic frequency *f* with units of hertz (Hz) [60].

$$f = \frac{\kappa c}{2\pi} \qquad \textit{(eq2.2)}$$

Similarly with respect to function *z* holding *t* fixed, we observe that the pressure around a particular time varies sinusoidally with a quantity *κ,* known as a wave number. We know wavelength of the sinusoidal wave is denoted as;

$$\lambda = \frac{2\pi}{\pi} \qquad \textit{(eq2.3)}$$

By substituting and solving *eq2.2 and eq2.3,* we yield an important relationship between speed of sound (*c*), frequency *(f)* and wavelength (*λ)* which is represented as

$$\lambda = \frac{c}{f} \qquad \textit{(eq2.4)}$$

For diagnostic purpose ultrasound wave frequency between 2MHz-15MHz is used. Generally low frequency ultrasound i.e. 2-4MHz is used for imaging deeper structures because of deeper penetration (like 10cm deep) but has low resolution. These low frequencies are used in Doppler system for fetal monitoring. Much lower part of ultrasonic spectrum is also used for surgical applications. Mid Frequency ranging from 5MHz-10MHz is used for imaging slightly deeper structure (like 5-6cm deep). Higher frequencies of ultrasound i.e. 10-15MHz are used for superficial structures (like 2 to 4cm) and have high resolution. Therefore, they are used in specialized application such as ophthalmology, skin imaging and intravascular investigation. Depending upon the area to be imaged operator sets the frequency for better resolution.

2.3 Ultrasound-Tissue Interaction

The interaction of ultrasound with tissues over a selected area of interest produces the desired information for diagnostic or therapeutic purposes. Generally, a beam of ultrasound is directed into the selected tissues and the ultrasonic energy would then

interact with the tissues along the path. As the ultrasound waves travel through the tissues, there would be some amount of waves which would be transmitted into deeper structures and other amount of waves would be reflected back to the transducer as echoes, some of it scattered and some of the waves transformed to heat.

Generally the echoes reflected back to the transducer are considered for imaging purposes. The property of 'Acoustic impedance' best describes the amount of echo returned after hitting a tissue interface. This medium property is referred to as the "Characteristic acoustic impedance of a medium". It is in a way a measure of the resistance of the particles of the medium to the mechanical vibrations. The acoustic impedance (Z) is defined as the product of medium density and ultrasound velocity in the medium.

$$Z = Density * Velocity \qquad (eq2.4.1)$$

Absorption coefficient (not be misunderstood with attenuation coefficient) is a term used for measuring the attenuation due to conversion of acoustic energy to thermal energy. This directly depends on frequency such that,

$$\alpha = a f^{b} \qquad (eq2.4.2)$$

The Table 2.1 below gives the acoustics impedance, speed of sound and Frequency dependence on absorption coefficient of various body tissues and organs, and also air and water for comparison.

Table 2.1: Acoustic Properties of Different Body Tissues and Organs

Material	Density (ρ) in kg/m^3	Speed (*c*) in m/s	Acoustic impedance (z) in Kg/m^{2}s	Frequency dependence (a=α/f) in dB/cm Mhz (assuming b=1)
Air	1.2	330	0.0004	12
Water	10000	1484	1.5	0.0022
Blood	1060	1570	1.62	0.18
Bone	1350-1800	4080	3.75-7.38	20.0
Brain	1030	-	1.55-1.66	0.5-2.5
Fat	920	1450	1.35	0.63
Kidney	1040	1560	1.62	1.0
Liver	1060	1570	1.64-1.68	0.94
Muscle	1070	-	1.65-1.74	1.0-3.3
Lung	400	-	0.26	41.0

The interaction of ultrasonic waves with different body tissues confronted along its beam can be described in terms of the following concepts.

- Attenuation
- Reflection
- Refraction
- Diffraction

2.3.1 Attenuation

The energy loss which happens when the ultrasound beam travels through the tissue layers is called attenuation. As the depth of penetration increases, the amplitude of the transmitted ultrasound wave becomes weakened. This energy loss or attenuation mainly occurs due to

- Absorption of ultrasound
- Scattering at interfaces

2.3.1.1 Absorption of Ultrasound

The process by which the energy in the ultrasound beam is transferred into a propagating medium where it is transformed into a different form of energy like heat is called absorption. Most of the energy from the beam is said to be absorbed by the medium. The extent of absorption however is dependent of different variables like frequency of the beam, viscosity of the medium and the relaxation time of the medium.
The measure of the frictional forces between particles of the medium as they move past one another describes viscosity. The amount of heat generated by the vibrating particles would increase with increase in the frictional forces. Hence, the absorption of ultrasound increases with the increasing viscosity.

The frequency of the beam also plays a key role in determining the absorption of the ultrasound. If the frequency of vibration is higher there would be more frictional heat. Increased frequency will reduce the probability of ultrasonic pulse or vibrating particles being reverted back to their equilibrium positions before the next disturbance. Since this increases the energy absorption, we can say that the absorption ultrasound increases with the increase in the beam frequency.

The time taken by the medium particles to revert to their original mean positions within the medium due to the displacement caused by an ultrasound pulse is known as the "Relaxation time". The value of the relaxation time is mainly dependent on the medium. When the relaxation time is short, vibrating particles revert to their original positions before the next pulse. When the relaxation time is long, the particles would not revert to their original positions before next pulse and so the next pulse may encounter the particles on its route before they are fully relaxed. This results in additional dissipation

energy from the beam as there would be new compression and the particles would be moving in opposite direction. Therefore the absorption of ultrasound would be increasing with increase in the length of the relaxation time. Longer the relaxation time, higher the absorption of ultrasound.

2.3.1.2 Scattering at Interfaces

Scattering of an ultrasound beam describes the spreading out of the beam energy as it moves away from the source. The Huygens principle of wavelets provides theoretical explanation for the spreading out of beam energy. Scattering affects the intensity of the beam both axially along the beam direction and perpendicularly, i.e. lateral to the beam direction. Interferences can either result in strengthening or weakening of the wave depending on the phases of interacting wave fronts. In the diagnostic ultrasound, the image resolution is greatly dependent on the dimensions of the ultrasound beam, manner in which the beam scatters and on the depth of the tissue.

The attenuation in specified mediums may be quantified in terms of the ultrasonic half value thickness (HVT). The ultrasonic half value thickness (HVT) of a beam of ultrasound in a specified medium is the distance within that medium which reduces the intensity of the beam to one half of its original value. Generally in soft tissues, absorption causes the attenuation of the ultrasound results in thermal effect such as undesirable heat production. The unit of attenuation is decibels per centimeter of tissue and is defined by attenuation coefficient. Higher the attenuation coefficient, higher would the attenuation of the ultrasound wave. For instance, bone has a high attenuation coefficient and thus it severely limits the beam transmission increasing the attenuation of the ultrasound wave.

Table 2.2 . Ultrasonic Half Value Thickness (HVT) for Different Material at Frequency of 2 MHz and 5 MHz

Material	At 2Mhz	At 5Mhz
Muscle	0.75	0.3
Blood	8.5	3.0
Brain	2.0	1.0
Liver	1.5	0.5
Soft tissue	2.1	0.86
Bone	0.1	0.04
Water	340	54
Air	0.06	0.01

The amount of attenuation depends on the frequency of the ultrasound wave and the total distance traveled throughout its transmission and reception. Generally speaking, a higher frequency ultrasound wave usually is correlated with higher attenuation thus limiting penetration through tissues, whereas a low frequency ultrasound wave has low tissue attenuation, resulting a deep tissue penetration. Based on this property the correct frequency range must be chosen for appropriate imaging. The Figure 5 below compares the attenuation degree in various biological tissues such as blood, liver and muscle.

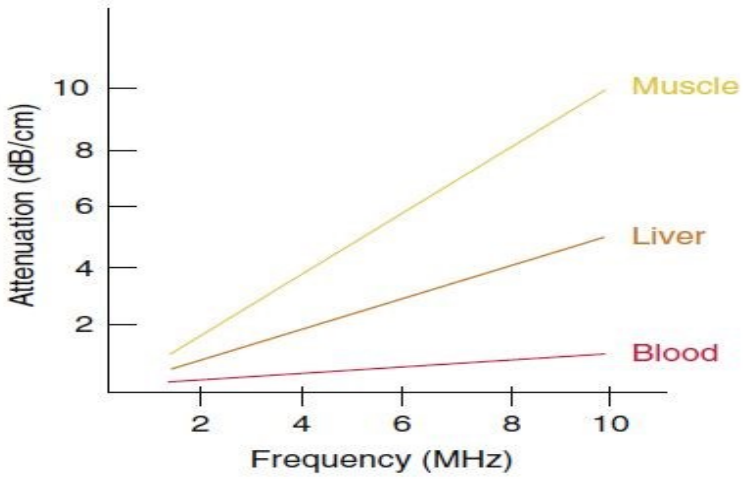

Figure 5: Comparison of Attenuation in Different Biological Tissue

2.3.2 Reflection

Reflection is the most important single interaction process for the purposes of generating an ultrasound image. A refelction of ultrasound beam when it encounter the interface is called an echo and the detection and production of echeos form the basis of ultrasound. A reflection occurs due to the property of acoustic impedance which is the product of the density and the propagation speed. For an echo to be produced, the acoustic impedance of the two materials should be different. If the acoustic impedance of the two materials is same, their bounday will not produce an echo. If the acoustic impedance of the two body materials is small then a weak echo will be produced , where as, if there is large difference in the the acoustic impedance of the two materials, all the ultrasound is observed to be totally reflected. Generally in soft tissues, most of the ultrasound wave is easily transmitted through the boundary and only a small percentage of ultrasound waves the echoes back, where as areas containing high reflecting material such as bone or air filled cavities can produce such large echoes such that its not enough to transmit and ultrasound limits to image beyond the tissue interface.

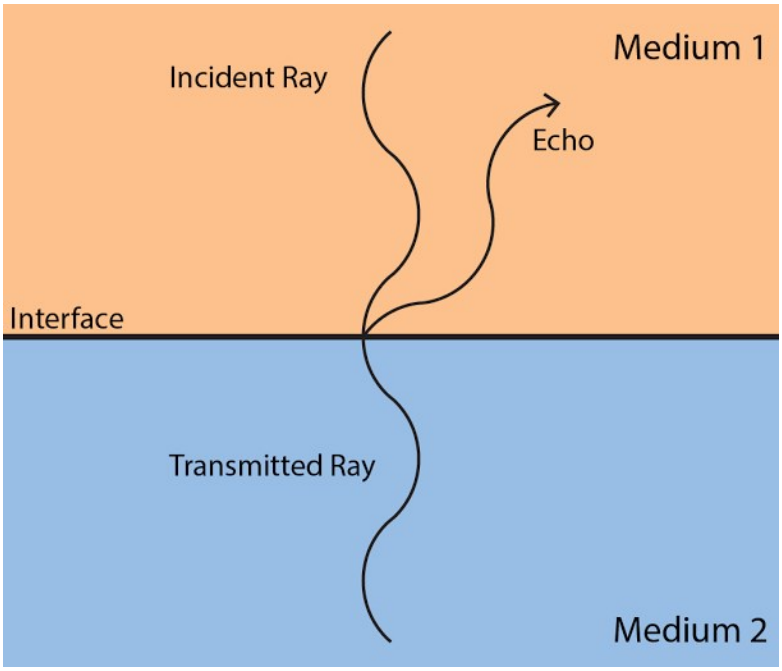

Figure 6: Production of Echo While Transmitting Through One Medium to Another

Generally there are two types of reflection that can occur depending on the size of the boundary relative to the ultrasound beam and on the irregularities of the shape on the surface of the reflector.

- Specular reflections
- Non-Specular reflections

The specular reflections occur when the boundary is smooth and larger than the dimensions of the ultrasound beam we would be dealing with. The Non-specular reflections occur when the interface is smaller than that of the ultrasound beam.

2.3.2.1 Specular Reflections

As shown in the figure, for specular reflection the law governing the reflection of light is obeyed. The angle 'i' between the incident ultrasound beam and perpendicular

direction to the interface is known as the 'angle of incidence'. The 'normal' to the reflecting surface is the line perpendicular to the interface. The reflected ultrasound beam would be opposite to the normal and the angle it makes with normal is known as the 'angle of reflection', r.

For specular reflection: The angle of incidence = the angle of reflection.

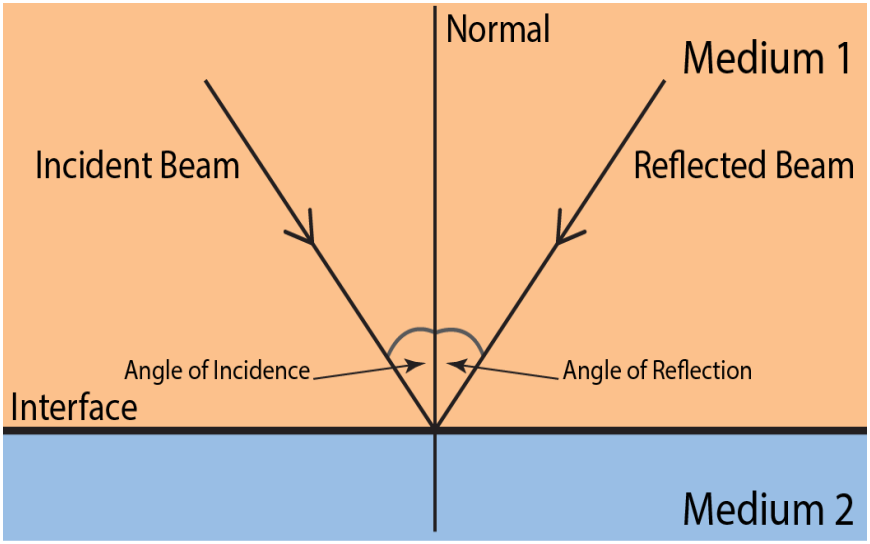

Figure 7: Specular Reflection

The probability than an reflected beam referred to as an echo would go back to the transducer and be detected increases as the angle of incidence *'i'* and angle of reflection *'r'* decrease. Typically if the angle of incidence is less than about 3°, the detection of an echo by the same transducer producing the incident beam is observed to be possible. The intensity of an echo due to the specular reflection depends on both the angle of incidence as well as the difference in acoustic impedance values of the two materials forming the boundary. This is also called as the acoustic mismatch. This difference is represented in *Z* value. When the ultrasound beam strikes the reflector at 90° angle, the angles of *'i'* and *'r'* are equal to zero and the reflected beam or the echo goes straight back with a higher probability of being picked up by the transducer. This is known as 'normal incidence'

and the intensity of the echo in relation to the intensity of the ultrasound beam incident upon the boundary is given by the following relation.

$$R = \frac{I_r}{I_i} = \frac{(Z_1 - Z_2)^2}{(Z_{1+}Z_2)^2} \qquad \textit{(eq2.4.3)}$$

R is the reflection coefficient measured as ratio of intensity of reflected echo I_r to intensity of incident beam I_i at the interface. This can also be rewritten in terms of acoustic impedance of first medium Z_1 to the acoustic impedance of the second medium Z_2 as shown in the equation above. It can be inferred that the difference in Z-value at the interface determines the reflection coefficient. A small change in Z value would produce small echoes as the reflection coefficient would be small. Similarly, a large change in the Z value at the interface makes the reflection coefficient large and there would be a large echo. This is a very important inference in ultrasound imaging. The following table shows the value of Z for some materials of interest in diagnostic and therapeutic ultrasound fields.

Table 2.3. Percentage Reflection of Ultrasound at Boundaries

Boundary	**% reflected**
Fat/Muscle	1.08
Fat/Kidney	0.6
Fat/Bone	49
Soft tissue/Water	0.2
Soft tissue/Air	99

As shown in the Table 2.3 above, at a tissue–air interface, 99% of the beam is reflected, since the beam is almost completely reflected it is difficult for further imaging. Therefore, transducers must be directly coupled to the patient's skin without an air gap. An ultrasound coupling gel or plain water can be used as a coupling medium between transducer and patient there by reducing resistance and undesirable attenuation.

2.3.2.2 Non-Specular reflections

When the reflecting interface is irregular in shape, and its dimensions are smaller than the diameter of the ultrasound beam, the incident beam is reflected in many directions. This is known as scattering or non-specular reflection. Unlike the specular reflections, the direction of scattering doesn't obey the law of reflection; it depends on the diameter of the ultrasound beam and the relative size of the scattering target. For the transducer to detect an echo, energy incident upon small target at large angles of incidence is desired. For scattering to occur, the dimensions of the interface should be about one wavelength of ultrasound beam. The wavelengths for typical diagnostic beams are 1mm or less. When used for diagnostic purposes on tissues and other organs, there are many structures within an organ with the wave length 1mm or less, these non-specular reflections or scattered ultrasound provides useful information in studying the internal texture of the organs. Generally the echoes from the non-specular reflections are weaker than the specular reflection echoes but because of the high sensitivity of the modern ultrasound equipment, it is possible to use the specular reflections for ultrasound imaging.

2.3.3 Refraction of Ultrasound

The change of the ultrasound beam direction at a boundary between the two materials or media in which ultrasound travels at different velocities is known as refraction. It can also be assumed as the change of the direction of the ultrasound wave on being targeted upon a tissue interface at an oblique angle. Refraction is mainly causes by a change of wavelength as the ultrasound crosses from one medium to the other while the frequency of the beam remains unchanged.

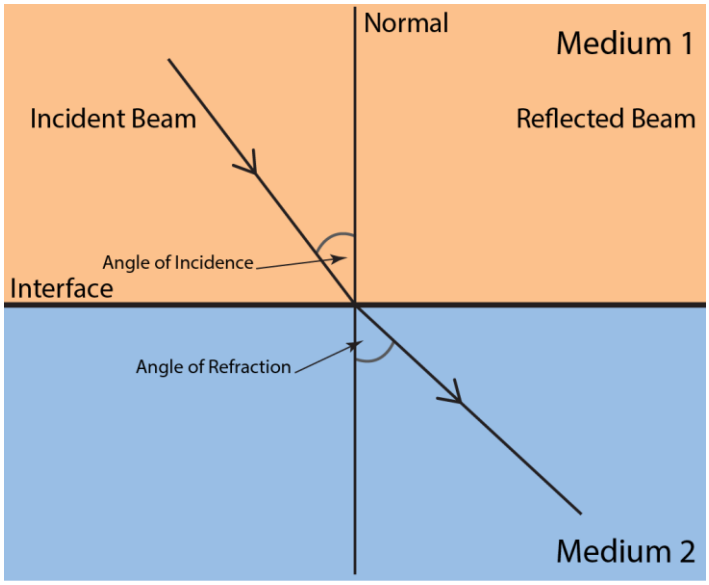

Figure 8: Refraction of Ultrasound

The Figure 8 explains the phenomenon of refraction. Refraction can only occur when the angle of incidence at the boundary is not zero. In case of normal incidence, part of the beam energy is reflected directly backwards, and the remaining energy transmits into the other medium without any change in the direction. At any other angle of incidence other the angle of normal incidence; the transmitted beam is deviated from the original direction of the incident beam, either towards or away from the normal. It depends on the

relative velocities of the ultrasound in the two media. Let velocity of ultrasound in medium 1 is V_1 and velocity of ultrasound in medium 2 be V_2, and then the relationship between the angle of incidence I and the angle of refraction R is determined by the Snell's law. Refraction doesn't contribute much for the process of image formation.

$$\frac{Sin\ I}{Sin\ R} = \frac{V_1}{V_2} \qquad \textit{(eq2.4.4)}$$

When ultrasound waves are targeted on the body through an ultrasound transducer, they penetrate through the body and interact with different body tissues and causes the waves to reflect or transmit or diffract, etc. back to the transducer. If the angle of incidence is perpendicular or close to perpendicular, maximum ultrasound waves are reflected back to transducer which means less attenuation and better image quality. If the ultrasound waves are parallel to the body, the resultant image would have less definition. Thus by adjusting the angle of incidence, the quality of image can be improved. These ultrasound- tissue interactions help in analyzing the modes and working principle of USCT. State of art of USCT architectures, modes and its imaging procedures are discussed in the following sections.

2.4 Ultrasound Computed Tomography

Ultrasound computed tomography (USCT) involves ultrasound imaging using computed tomography methodology. One can imagine USCT as an imaging procedure where X-rays in a CT scanner are replaced by ultrasound waves. Therefore, to image an object of interest a burst of ultrasound waves are targeted on the object through a coupling medium and simultaneously, the receivers captures the sliced images (outgoing signal) and then reconstructs back into detailed image using computer software tools for better diagnosis. USCT has can eliminate the possible drawbacks of conventional

ultrasound imaging such as operator dependent output and low resolution. USCT provides high resolution images without using any radiation. It can be consider as a safe imaging technique.

The main component of USCT is ultrasound transducers (Single transducer or array of transducer) that can be arranged in ring shape or linear fashion or free handed too. These transducers transmit sound waves and also receive the sound waves back in form of echoes. The other general components include a pulse generator, amplifier, digital oscilloscope and computer. The architecture of USCT varies according to the transducer arrangements. There are several ways of arranging the transducers based on one's requirements. In this thesis, all the transducers are marked as T/R, which implies these can be used as transmitter or receiver. Figure 9 shows the several proposed architectures of USCT based on transducer placement [1]. Fig 9.a. shows a simplified model of ultrasound tomography which has two transducers that can be rotated readily around the object. In Fig.9.b the transducers are arranged in ring shaped array enclosing the object. Fig.9.c. shows the arrangement in which the transducers are aligned as two linear opposite array rotating mechanically around the object.

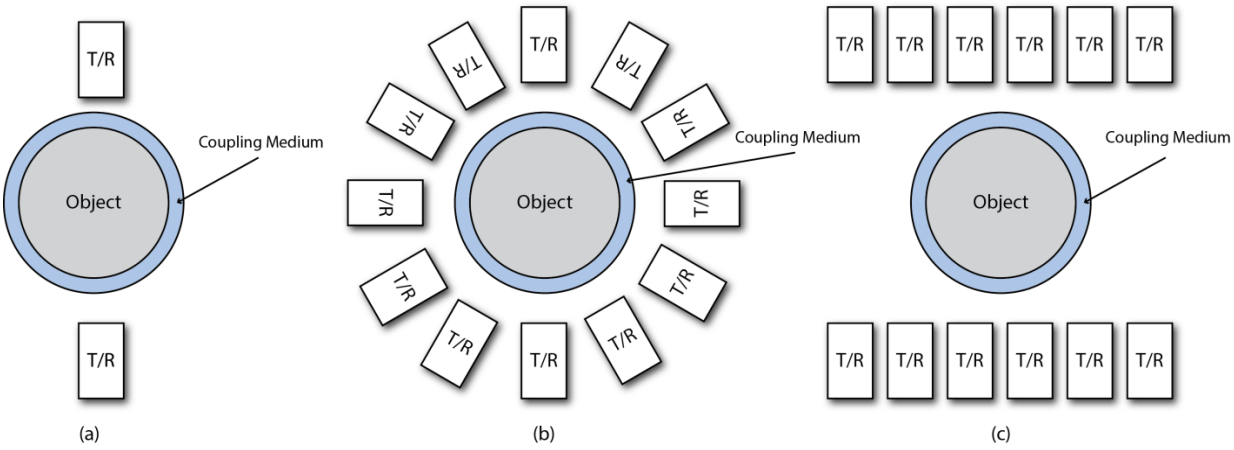

Figure 9: Different Transducer Arrangements

Due to high complexity and high data transmission rate, approx. 100 Gb/sec, these USCT are still not commercially in use. These systems are not portable, in contrast to the conventional ultrasound imaging system.

Also, USCT mostly uses an array of transducers and as the number of transducers increases the cost of equipment increases making USCT system no longer economical. Customarily ideal number of transducers used for a ring shaped arrangement can be 36 that have a beam, divergence angle of 70 degrees [16]. A better reconstruction quality is the achieved by widening the beam angle of the ultrasound transducer without expanding the number of transducers too. Therefore, lot of research the progressing toward these drawbacks and trying to implement an ideal standard practical Ultrasound computer tomography. But we aim at first reducing the complexity and time consuming reconstruction methods.

2.5 Basic USCT Projection Principle

Ultrasound computer tomography (USCT) aims at fast high resolution 3D imaging. The basic principles behind any, ultrasound tomography scanner are standard,

but the approach may change. Firstly, a mathematical model describing the tissue-sound interaction and parameters of interest is deduced.

2.5.1 Mathematical Model

In USCT system, the ultrasound waves are directed into a body through a coupling medium like water or gel, which attenuates negligibly with a uniform coefficient of attenuation α_{water} and can yield a projection image. For example, consider projection onto (*x, z*) plane, then projection image *P(x, z)* can be represented mathematically [18] as;

$$P(x, z) \triangleq \int_{-\infty}^{\infty} f(x, y, z)dy \qquad (eq2.5)$$

Where *f (x,y,z)* is the desired object to be scanned. Let us consider *P(θ,s)* as a 1-D projection at an angle *θ*. Assuming the object is illuminated with an appropriate field along the line integral *l* . *P (θ,s)* is the line integral of the image *f (x,y),* along the line that is at a distance *s* from the origin and at angle θ of the x-axis.

$$P(\theta,s) = \int_{l} f(x, y)dl \qquad (eq2.6)$$

We all know all points on this straight line satisfy the equation *xsin (θ) – ycos (θ) = s*. Therefore, the projection function *P (θ,s)* can be rewritten as;

$$P(\theta,s) = \iint f(x, y)\delta(xsin\theta - ycos\theta - s)dxdy \qquad (eq2.7)$$

The collection of these *P(θ,s)* at all θ is called the Radon Transform of an image *f(x,y)*.

The Radon transform (RT) of a distribution *f(x, y)* is defined by

$$P(\theta, s) = \int f(x,y)\ \delta(xsin\theta - ycos\theta - s)dx\,dy, \qquad (eq2.7.1)$$

The Sinogram p(s,θ) has many essential mathematical properties, an important one of which is

$$P(s, \theta) = p(-s, \theta + \pi) \qquad (eq2.7.2)$$

The task of the tomographic reconstruction is to find $f(x, y)$ given knowledge of $p(s, \theta)$.

If sufficient set of these collected data is available then reconstruction is readily preformed with the procedures below.

2.5.2 Reconstruction Algorithm

Reconstruction is an approach is an essential method in imaging which is meant to reconstruct or extract back the feature space from the obtained projection. The basic reconstruction method is the inversion of radon transform. This inversion is the solution of the problem of "reconstruction from projections" when the projections can be interpreted as the Radon transform of some function in feature space. The solution to the inverse Radon transform is based on the projection slice theorem (PST) also known as Central slice theorem (CST) which) is the basis for Fourier-based inversion techniques explained by Swindell and Barrett [55]. The CST theorem states that the value of two dimensional Fourier transform of '$f(x, y)$' along a projection line at angle θ is given by the one dimensional Fourier transform of '$f(p,\theta)$', the projection profile of the sonogram acquired at angle θ. CST related $F(u,v)$ which is the Fourier transform of '$f(x, y)$' and $F(\xi,\eta)$ of the Fourier transform of '$f(p,\theta)$'.

Mathematically, the PST is defined by [55],

$$F(\xi,\eta) = F(p\cos\theta, v\sin\theta) \qquad (eq2.8)$$

A tomographic cross-sectional image of the object can be obtained, using "projection slice theorem." Using projection slices obtained, an image can be reconstructed.

Reconstruction of the projected data is necessary for obtaining an image with high resolution. There are many reconstruction techniques one such is the Back projection reconstruction approach [56]. This is the basic reconstruction technique. As the name implies, it means to simply run the projections back through the image to obtain an approximation to the original image. That is the projections will simply interact the measured Sinogram back into the image space along the projection paths. Mathematically, the back projection of the line integral along a line at an angle θ and distance 's' can be defined as [55]

$$f_{BP}(x,y) = \int_0^{\pi} p(x\cos\theta + y\sin\theta)d\theta \qquad \textit{(eq2.9)}$$

Once F (u,v,) is obtained from f(p, θ) using the PST, f(x,y) can be obtained by applying inverse FT to F(ξ,).

The back projection method is practically not feasible. Hence on introduction of a ramp filter, the reconstruction is more efficient. This approach is named as the filtered back projection algorithm (FBP). Considering *F(u,v)* which is the Fourier transform of '*f(x, y)*' and *F(ξ,ŋ)* of the Fourier transform of *'f(p,θ)'* then filtered back projection [56] can be derived as follows;

$$\text{F(x, y)} = \int_{-\infty}^{\infty}\int_{-\infty}^{\infty} d\xi\, d\eta\, F(\xi,\eta)e^{-j2\pi\xi x}e^{-j2\pi\eta y} \qquad \textit{(eq2.10)}$$

$$= \int_0^{2\pi} d\theta \int_0^{\infty} dp\, p\, F(p\cos\phi, v\sin\phi)e^{-j2\pi\xi\cos\phi}\, e^{-j2\pi\eta\sin\phi} \qquad \textit{(eq2.11)}$$

$$= \int_0^{2\pi} d\theta \int_0^{\infty} dp\ P(v,\phi)e^{-j2\pi v(x\cos\phi+y\sin\phi)} \qquad \textit{(eq2.12)}$$

Using equation $f(p,\theta+\pi)$ = F(-p, θ), we have

$$\int_{\pi}^{2\pi}\int_0^{\infty} v\, P(v,\phi)e^{-j2\pi v(x\cos\phi+y\sin\phi)}d\theta\ dp \qquad \textit{(eq2.13)}$$

$$= \int_0^{\pi}\int_0^{\infty} p\, f(p,\theta)e^{-j2\pi v(x\cos(\theta+\pi)+y\sin(\theta+\pi)}dp\ d\theta \qquad \textit{(eq2.14)}$$

$$= \int_0^{\pi} \int_{-\infty}^{0} (-p)\, f(p,\theta) e^{-j2\pi v(x\cos\theta + y\sin\theta)}\, dp\, d\theta \qquad \textit{(eq2.15)}$$

Therefore,

$$f(x,y) = \int_0^{\pi} \int_{-\infty}^{\infty} |p| f(p,\theta) e^{-j2\pi v(x\cos\theta + y\sin\theta)} dp d\theta$$

$$= \int_0^{\pi} F'(x\cos\phi + y\sin\phi)\, d\theta \qquad \textit{(eq2.16)}$$

Where

$$F'(\xi, \phi) = \int_{-\infty}^{\infty} |p| F(p,\theta) e^{-j2\pi v\xi} dp \qquad \textit{(eq2.17)}$$

$$= f(p,\theta) * b(\xi) \qquad \textit{(eq2.18)}$$

Hence, f(x,y) can be obtained by back projection of $p'(\xi,\phi)$ [56]

Initially, the algorithms followed for reconstruction techniques are of the filtered back propagation type [20] or simply inverse Fourier transforms [21]. These algorithms are iterative in nature. They suffer from excessive computing times. Later in 1994, approach based Sinc inversion of the Helmholtz equation without computing the forward was tested numerically [22]. The most alternative promising approach was back propagation method suggested by Frank Natterer and Frank Wiibbelmg [23].

Though there are different techniques of reconstruction, the basic principle remains the same. Consider a USCT system with transmitter and receiver rotating with angle θ around the object and obtains projection images along the line of integral in a data matrix (Sinogram matrix) format. These projections are collected by repeating the scan for all the sonogram rows in the 2D Fourier domain. These projections are interpolated into a Cartesian matrix. The resulting image is obtained by applying inverse Fourier transform to the measured matrix of the 2D Fourier values. The flow chart below depicts the step by step process of basic reconstruction.

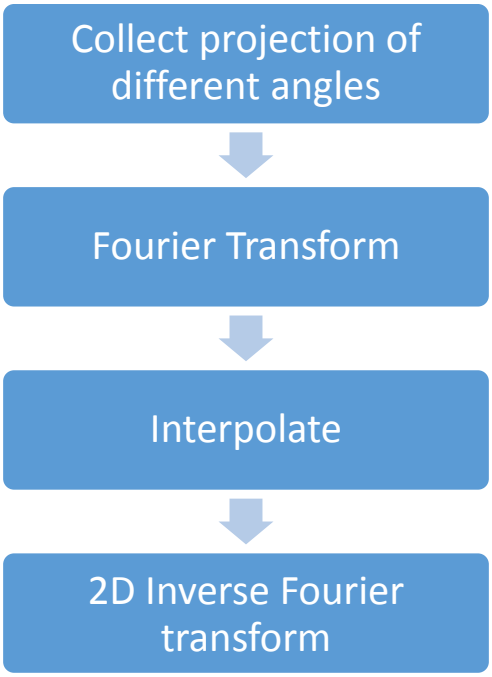

Figure 10: Flow Chart for Image Reconstruction

Many reconstruction techniques incorporate a filter for image enhancing. In Filter back projection method (FBP), a 2D low pass filter whose value in Fourier domain is given by |k| is used. Other techniques like algebraic reconstruction tomography (ART) methods are also efficient and robust. The image projection data and reconstruction techniques together are responsible for a desired scanned object. Hence understanding the techniques and utilizing the best suited techniques is much needed for creating a best ultrasound simulation.

2.6 Ultrasound Computed Tomography Modes

Ultrasound tomography models in specific are slightly different from those in x-ray tomography models. Unlike X-rays, ultrasound waves do not travel in a simple straight line, it undergoes multiple deflections too. Also, propagation speed of ultrasound is low, such that delay in propagation times can also be measured. Various methods have been suggested to deal with these refractive problems. All together these methods can categories ultrasound computer tomography under three modes;

- Transmission mode
- Reflection mode
- Diffraction mode

Transmission tomography mode images the velocity (acoustic speed) or attenuation in the medium, while Reflection tomography mode images the ultrasonic reflectivity. USCT in diffraction mode uses inverse scattering solutions to form images. Diffraction mode tomography uses an alternate approach compared to transmission or reflection mode tomography, known as inverse scattering problem for reconstructing the parameters of interest. These modes are explained in detail below.

2.6.1 Transmission Mode Tomography:

To the best of our knowledge, James F Greenleaf was the first who has come up with the idea of transmission tomography. Greenleaf et al. have worked on reconstruction of the acoustic attenuation coefficient to map the image [25]. Several other researchers later explored mapping with attenuation coefficient or speed of sound or any other means for the reconstruction and also tried to test the clinical applicability [26] [27] [28].

In general, the projection image of the object of interest with USCT in transmission mode can be made by either comparing the amplitude of the pulses which is used to reconstruct the acoustic attenuation or to use time-of-flight (TOF) measurement which then used to reconstruct speed of sound (SOS). The following transmission tomography model in Figure 11 explained below defines the line integrals of these two parameters i.e. acoustic attenuation and speed of sound in terms of the measured quantities.

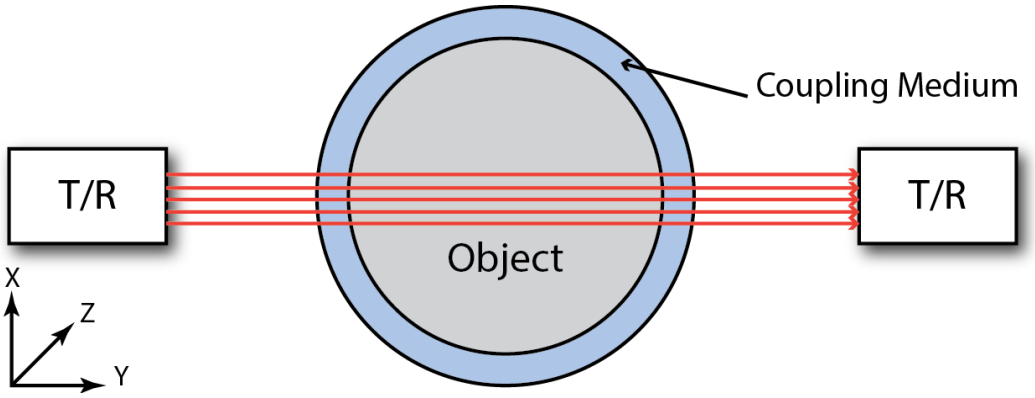

Figure 11: Depiction of Transmission Mode of USCT

Let us consider, in transmission method, the organ to be scanned is coupled with a coupling medium and placed in the center. The transmitter (Figure 11) and the receiver are positioned opposite sides to each other; such that the object is insonified with a beam of ultrasound along a line from the transmitter and receiver detects the transmitted ultrasound simultaneously to obtain a projection image. The Ultrasound wave is assumed to travel along a straight line L along line of sight and generally used protocol for scanning is a raster scan.

The travelling time of the ultrasound from one side to another i.e. travelling time of ultrasound waves from the transmitter to receiver through the medium is known as Time of flight (TOF). This TOF is used to measure speed of sound through that particular medium. In detail, the ultrasonic wave travels through coupling medium, consider water in this case and object and again through water and strikers receiver. The practical form of TOF equation is given below;

$$\int_L \left(\frac{1}{c(x,y)} - \frac{1}{c_w} \right) dl = TOF_{obj} - TOF_{water} \qquad \textit{(eq2.19)}$$

Where $c(x,y)$ is the speed of sound through object, c_w is speed of sound through water, which is generally known to 1484 ms^{-1}. TOF_{obj} and TOF_{water} are the time of flight through

object and water respectively. Rewriting the above equation with valid assumptions and derivations into more generalized form we get, TOF_{obj} along *y* direction that is related to speed of sound of that particular medium;

$$TOF_{obj} = \int \frac{1}{c(x,y,z)} dy \qquad (eq2.20)$$

We know from optics and acoustic physics that the refractive index of the medium is defined as the reciprocal value of the medium speed of sound (SOS), which is $n=1/c$. The obtained image depicts the sum of all the indices along each integral line. The resulting image is a projection image. In the above case transmitter is holding in y direction; therefore, geometrical information along the integrated axis is lost. Therefore, projection from various directions is calculated and reconstructed into an image.

Another form of obtaining the image that depicts the average attenuation coefficient would be through comparing the measured amplitude of the transmitted ultrasonic wave through tissue. If the amplitude of the attenuated wave at a known distance l (distance from object to the transmitter) be $A°$, then the amplitude of the received wave $A(x,z)$ will be;

$$A(x,z) = A°.e^{-\int \alpha(x,y,z)dy} \qquad (eq2.21)$$

where $\alpha(x,y,z)$ is the attenuation coefficient. Dividing both the sides of equation by amplitude of transmitted wave and taking logarithm, the equation becomes;

$$\int \alpha(x,y,z)dy = ln \left| \frac{A(x,z)}{A°} \right| \qquad (eq2.22)$$

Assuming the dimensions of the object and l and a reference scan is performed under water (no object) denoted by y_{water} and the measured wave is denoted as $y_{obj.}$ On solving equations above and rearranging it [26], we get;

$$\int \alpha(x,y,z)dy = ln \left| \kappa^{\circ} \frac{Ywater}{Yobj} \right| \qquad (eq2.23)$$

Where $\kappa^{\circ}=e^{-\int \alpha(water)dy}$, is the attenuation coefficient of water which is practically negligible.

2.6.2 Reflection Mode Tomography

In reflection mode, ultrasound computer tomography works based on measurements of line integrals of the reflectivity of the object of interest. In 1977, Johnson et al. examined USCT in reflection mode using a computer simulation. But due to limited technology and other artifacts (such as mentioned in section 2.7) it faced many drawbacks [29].Norton et al. were quite successful to put forward theoretical and experimental analysis of the reflection tomography where ultrasonic reflectivity measurements were carried out through scattering measurements based on scanning using circular arrays [30]. Kim at al. [31] has inspected refraction effect on ultrasonic reflectivity measurement. Dines and Goss in 1987 tried to test the feasibility of such mode in tissue cross sections using backscattered energy obtained by fan- beam and plane-wave pulse-echo interrogation [32]. The research still continues to reconstruct a quantitative cross- sectional image from reflection data to improve spatial resolution.

USCT working in reflection mode can be explained using a model in Figure 12. In this, let us assume the system works on single transducer and the object of interest are placed at a distance from the transducer. The transducer acts as both transmitter and receiver. When the transducer is excited by voltage, the object is insonified by ultrasound transducer forming a wide cone shaped beam. In the cone-beam case, circular-arc wave

fronts are produced, while, in the plane-wave case, the wave fronts consist of parallel straight lines. Now consider cone shaped beam which spreads out with circular-arc wave fronts, but is always focused perpendicularly to the image plane. If the transducer is excited at time *t=0* and speed of sound in the medium *c* is constant, then the acoustic pulse is detected at a distance *d= ct* from the source.

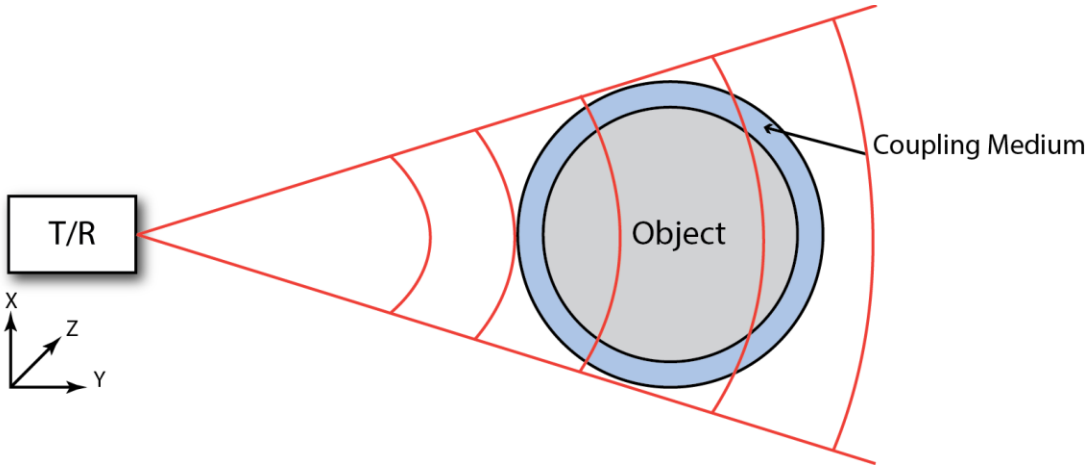

Figure 12: USCT Model in Reflection Mode Using Single Transducer

If the transducer is excited by impulse signal (practical approach), incident ultrasonic field is an impulse response of a linear system in the time domain. At specific time t and at a distance *d=ct/2* from transducer, the received signal *r (d)* at the output is the sum of total reflection. Then the backscattered signal received at time *t=2d/c* at angle θ during the time period *g* is the convolution of received reflection signal *r(t)* at distance *d* ; and reflectivity function *f (x,y,z)* and amplitude pattern of the transducer beam *a (x,y,z),* this can be represented as [30];

$$g_\theta(t) = r(t) * \int_l a(x,y,z) f(x,y,z) dl \qquad (eq2.24)$$

where l is the circular-arc line of integration. But sometimes part of the ultrasound undergoes multiple reflections at the boundary of tissues of different characteristic impedance. These reflected signals propagate back and detected again. The time difference between these multiple signals gives a picture about size of the tissue whereas the magnitude of the received signal corresponds to characteristic impedance or object reflectivity.

Consider the other case, where the transducer is excited by the waveform $p(t)$ forming cone shaped beam with the plane-wave fronts consisting of parallel straight lines, then the field produced by an ideal is[31];

$$\Psi_i(x,y,z) = p\left(t - \frac{2l}{c}\right) \qquad (eq2.25)$$

The received reflected signal $r(t)$ along the line of integration l can be written as;

$$r(t) = \int_{-\infty}^{\infty} p\left(t - \frac{2l}{c}\right) f(l)\, dl \qquad (eq2.26)$$

Here $f(l)$ is the function of reflectivity along the line l. The reconstruction of the image is carried out through acoustic back projection method or Fourier slice theorem. The one of the main drawback of Ultrasound computed tomography is it lacks resolution and complex reconstruction methods. USCT in transmission mode or reflection mode consider ultrasound wave as a ray. In reality ultrasound is a kind of sound wave, which has properties of sound i.e. it does not travel in straight line unlike rays. Sound wave can scatter (diffract) too. Especially, when size of objects is much smaller than the wavelength of ultrasound, ray statistics cannot be applied. Applying ray statistics for

ultrasound wave loses the essential components or details of the images. Hence in case of ultrasound study, diffraction theory is necessary.

2.6.3 Diffraction Mode

When Ultrasound penetrates through an inhomogeneous medium, it undergoes diffraction and creating a scattered pressure field in the output. The characteristic of the scattered field reveals the tissue property. This scattered field forms the base of the ultrasound diffraction tomography. USCT in diffraction mode can be referred to as analogy to reflection tomography where instead of summing all the received signals, each one is separately recorded and reconstructed taking the Fourier transform of each received signal with respect to time.

Diffraction mode tomography uses an alternate approach known as inverse scattering problem for reconstructing the parameters of interest. Tomographic reconstruction in diffraction mode uses inverse scattering approach also known as forward scattering problem. Commonly scattering problem is solved with Lippmann-Schwinger or Integral equation using Green's function. Iwata and Nagata [33] were first to bring in the idea of ultrasonic tomography where they calculated refractive index distribution of object of interest using the Born and Rytov's approximation. Later, Mueller et al. and Stenger et al. investigated on this method through various reconstruction algorithms [34] [35]. Many computer simulations testing these methods have met success but the not clinical applied till present. This diffraction mode tomography is discussed in detail in the following chapters. The aim of USCT in diffraction mode is to eliminate the resolution issues and improve the image quality. This

image quality can be improved with good reconstruction techniques and good suitable computational methods.

2.7 Image Quality and Artifacts

The ultrasound image quality can be described by two most important factors; spatial resolution and contrast resolution [16].

2.7.1 Spatial Resolution

The radial and lateral resolutions come under spatial resolution. Radial resolution also called axial resolution or depth resolution, could be defined as the closest distance between two objects along the propagation axis and displayed as two distant objects. And any objects with closer distance than the radial resolution will merge together in the image. It is expressed as ;

$$\Delta r = \frac{c\, P_L}{2} = \frac{c}{2\, A} \qquad \textit{(eq2.27)}$$

where P_L is pulse length, A is the pulse bandwidth and c is the speed in human tissue (1540m/s). The resolution is depends on the pulse length, a short pulse gives good radial resolution but decreases the depth of penetration. It also depends on the frequency and the bandwidth of the transducer number of pulse periods.

On the other hand, the lateral resolution is the closest distance between two objects transverse to propagation beam and are displayed as two distinct objects. This resolution is represented as

$$\Delta l = \frac{k\,(\lambda.F)}{A_p} = k\lambda f \qquad \textit{(eq2.28)}$$

where F is the focus, Ap is the aperture and k is a scaling constant. Lateral resolution is determined by the beam width at the focus point and frequency. Increasing the transmit frequency the lateral resolution is improved and the resolution will also be improved by small separation between the beams, where the scaling constant is dependent of the transducer shape.

2.7.2 Contrast Resolution

Contrast resolution is the lowest difference in the signal strength from adjoining structure that allows the observer to observe the structure as separate entities. This shows the ability to differentiate a weak target that is close to a strong one. A small in-homogeneity such as cyst contains a region in the image with no scatter which servers as good example of a weak target. A good Contrast is very easily readable, very high contrast or very low contrast is not idle for image quality. Sometimes defected echoes from random variation signal amplitude results to noise and causes brightness fluctuation in the ultra sound image. This noise and multiple reflections of the ultrasounds pulse limit the resolution of an image. Noise can be separated into two different types, electronic noise and acoustic noise. Electronic noise starts from amplifiers and cross coupling of cables, whereas acoustic noise results from side lobes and grating lobes. These kinds of noise generated by the transmitted signals are the main drawback of contract resolution. The contrast resolution is also called the local dynamic range of the image. This must not be misinterpreted with total dynamic range, which is a ratio of strongest signals from close target to weakest signal from very deep targets.

The sharpness of the tissue boundaries is associated acutance, which is with how quickly the transition at an edge is and it's closely related to spatial resolution. Sharpness

describes the ability of the scanner to create tissue boundaries. Acutance is a very useful parameter when determining the image quality but difficult to obtain in ultrasound images.

Temporal resolution refers to capacity to precisely visualize moving object and measure fastest detectable moving object. This resolution is restricted by frame rate, thus increased frame rate better the temporal resolution. And the same time decrease the lateral resolution or the image field.

Artefacts are the errors created in the output image that do not represent valid anatomical or functional objects. Artefacts are not desirable because they affect the image quality. Ultrasound imaging system works under many assumptions regarding speed of sound, attenuation rate, beam axis, echo time and transmission. For instance ultrasound assumes speed of sound through tissue is always 1540m/s, the rate of attenuation of the ultrasound wave is constant with depth and throughout the FOV, the transmission of ultrasound through medium is in straight line. But in reality these assumption differ creating artifacts in the output image. The other fact is ultrasound can be scattered and also absorbed by medium, therefore reducing the strength of the signal that reaches the detector. Most artifacts degrade the image quality and can lead to misdiagnosis, but the artifacts are at the same time inherent in the imaging process and cannot be totally eliminated.

2.7.3 Scanning Artifacts

Ultrasound passes through different mediums with different velocity. However some medium (fluids) allow ultrasound to penetrate through them much easily than others such as dense tissue or bone. Because only least percentage of energy is absorbed

by the fluid or semi-fluids, the region that lies beneath them will receive more sound than the system expects for that depth. Therefore, this area will appear uniformly brighter than expected. Such artifacts is called enhancement. The vice versa some medium may absorb more ultrasound and area lying beneath would appear dark or sometimes create a shadow. A classic example is when ultrasound is transmitted through soft tissue/gas interface or soft tissue/bone interface creating acoustic shadowing. During a real time imaging, some tissues appear to be bright but when the angle is changed it appears darker. This illusion builds up for a suspicious doubt of tear in the tissue. But this is due to anisotropy effect caused by theory of angle of reflection and incidence. This is the effect is more particular for smooth boundaries such as tendon which seem to show up bright when angle of incidence of ultrasound beam is 90 Degrees, but dark when the angle is altered.

These scanning artifacts are minimal for expert radiologists who have an eye to oversee these artifacts and still see a clearer image in their mind. Few other artefacts that are important to know are those artefacts reflected in images while scanning such as Mirror image artefacts, Comet tail artifact, range distortion artefact and beam width artefacts. Mirror images artefacts occur when the tissue to tissue interface lies within the FOV at an angle to the ultrasound transducer such that it causes structure like organs that lie in front or to the side of it, to appear as if they lie behind it. Here the interface acts like a mirror creating a virtual image of the real image. For example, a common mirror artifact that may show is the mirroring of liver texture above the diaphragm for a diaphragm/lung interface.

Reverberation is another artifact which is due to evenly representations of same interface at increasing depths and resultant caused by sound echoing backward and forward between the interface of the ultrasound transducer and a tissue acting as reflector lying close to the surface with every subsequent echo appears to be deeper because it has taken longer to get back to the ultrasound. This causes tiny bright streaks as it sequentially loses amplitude that is seen deep to the structure slowly diminishing in size as if it had a tail forming a "Comet tail artifact". Ultrasound travels at slightly different velocities through different tissues. Ultrasound is assumed to travel with a velocity of 1540m/s, but the velocity through fat (approximately 1450 m/s) and water (approximately 1480m/s) is somewhat slower. Organs lying beneath or deep to a large cavities or denser object like bones, can therefore appear a little further away than they actually are because different velocities of sound causes incorrect placement of the echoes in the display and thereby creating a range distortion artefact.

Usually Transducer cannot produce a wave that just travels in one straight focused direction, its side lobes consist of multiple low-intensity sound beams located outside of the main ultrasound beam too. The sides lobes are usually have weak intensity and so normally do little to degrade the image. The beam width, side lobe, grating lobe and slice thickness artefacts fall under this category. These artifacts occur near highly reflecting surfaces such as the diaphragm, or near large cystic masses such as the urinary bladder or gallbladder.

Other artefacts are twinkling artefact (TA) seen on color-Doppler ultrasound (US) especially during diagnosing urolithiasis and strip artifacts seen during diagnosis of acute

stroke or brain perfusion diseases. These artefacts are very uncommon but still contribute in image quality deterioration.

2.7.4 Bio-effects of Ultrasound

Ultrasound radiation in clinical use is known to, be less hazardous to the human body when operating under 'safe zone' conditions [25]. A plane low energy monochromatic ultrasonic waves can assumed to be as sinusoidal waves with high frequency number. As the intensity of the ultrasound increases it may displays few non-linear properties which tend to lead to bio-effect such as increased absorption, streaming and cavitation. These bio effects are very minimal and rare in normal ultrasound imaging (not while using as a therapeutic tool). These could be a problem when left unattended due to improper care and attention.

Absorption can be considered as thermal bio-effect. If a tissue is exposed to ultrasound for a long period of time, it absorbs more ultrasound, resulting in heating up of tissue. The amount of heating is directly dependent on the frequency and amount of intensity of the ultrasound (i.e. the dosage). Streaming and cavitation are the non-thermal bio-effects [51] which lead to "injures to the cell and subsequently resulting in growth retardation. The physical forces of the ultrasound waves while transmitting through a medium containing fluids would provide a driving force capable of displacing ions and small molecules within the medium and may produce eddy effects known as streaming. A more dramatic non-thermal bio-effect is "cavitation". This is where tiny collections of gas, known as microtubules oscillate in response to the ultrasound wave causing them to

enlarge and then spontaneously explode. The resultant release of energy has a potential to harm delicate structures around the soft tissue.

3 Chapter: USCT in Diffraction Mode

Diffraction of sound waves can be defined as bending of sound waves caused by an obstacle in their path or past a small opening. The diffraction of sound waves occurs when the size of the object is smaller than the wavelength. The mechanism of diffraction of sound waves can be well imagined to analogous to water waves that have the ability to travel (bend) around an obstacles or corner and through an opening. Ripples which are created in water tank bounces off the wall (Reflection). If we place a stick which has diameter smaller then length of ripples in their path, then the ripples bends around the stick and continue their path. This deflection of ripples is due to diffraction property. The Figure 13 picturizes the mechanism of diffraction of sound waves due to presence of a scattering object.

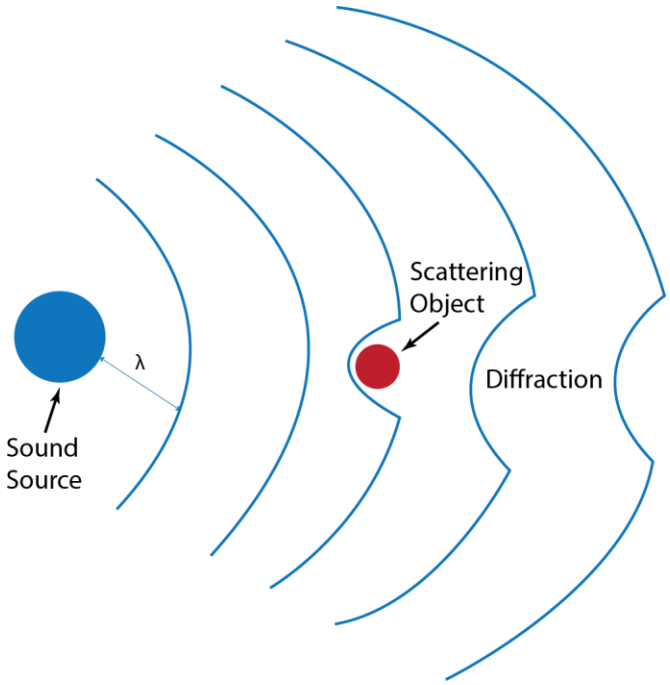

Figure 13: Diffraction of Sound Wave

Due to diffraction of sound waves, we can hear the sound from one room to another. Similarly, ultrasound waves also undergo diffraction and this diffraction nature of ultrasound account for details of the materials in which it transmits through. Many birds especially forest habitants take advantage of this diffractive ability of ultrasound waves. Bats for example, use ultrasound waves in order to improve their ability to hunt their prey. Bats use the physics of ultrasound waves to detect the presence of their prey (insects) around them. They create ultrasound waves with wavelength typically 50,000 Hz which are transmitted through air. As these ultrasound waves hit the target i.e. their prey (typically few centimeters in length), they reflect back by means of echolocation instead of diffraction around the prey. But this is unlikely in case of objects smaller than ultrasound wavelength i.e. smaller than few centimeters.

Consider 2MHz frequency of ultrasound travelling in a soft tissue with speed 1540m/s. Then the wavelength of ultrasound can be calculated as (according to *eq2.4*)

$$\lambda = \frac{c}{f} = 1540/2\text{MHz} = 0.7\text{mm}$$

If the same tissue has a cyst of 0.5mm in diameter, then ultrasound wave diffracts. This diffraction nature indicates the presence of cyst (small object) in the tissue. These small objects provide the minute details of the object on interest. On the whole this diffraction phenomenon of ultrasound waves cannot be ignored as it gives more précised details and also accounts for the resolution of the object.

An ultrasound computed tomography which considers the diffraction property of ultrasound is said to be working in diffraction mode. When Ultrasound penetrates through an inhomogeneous medium, it undergoes diffraction due to scattering term and creating a scattered field in the output. The formation of scattering field can be visualized

in the figure below (Figure 14), when the object of interest is insonified by ultrasound plane waves. The characteristic of the scattered field reveals the tissue property. This scattered field forms the base of the ultrasound computed tomography in diffraction mode.

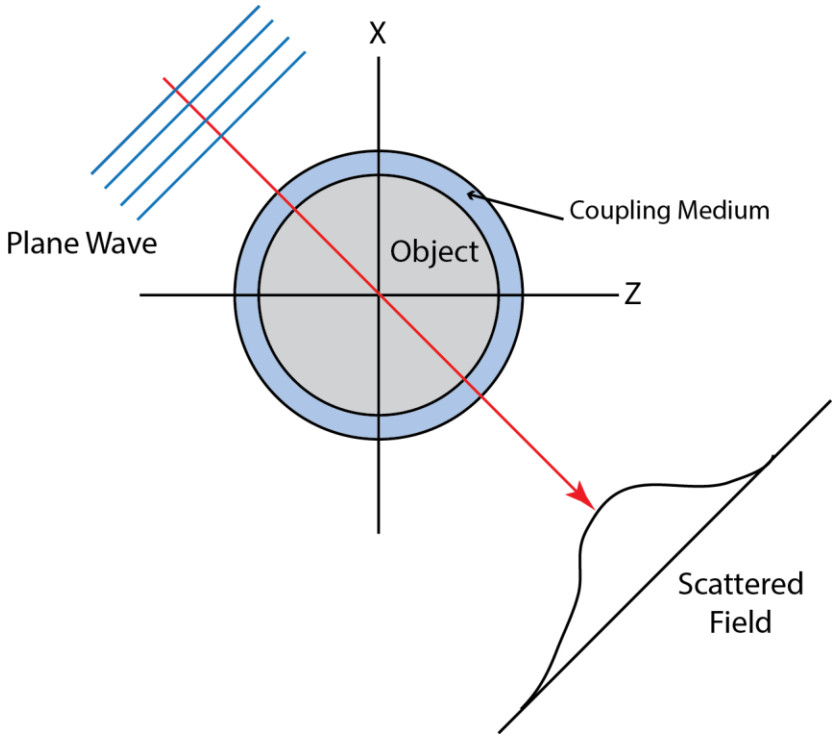

Figure 14: Object Producing Scattered Field when Insonified under Plane Wave

The essential components of ultrasound diffraction tomography are, firstly, a mathematical model describing the tissue-sound interaction and parameters of interest. Secondly,a reconstruction procedure to deduce the parameter of interest from the measured solutions.

In this chapter, we address problems of ultrasound tomography in terms of mathematical wave models describing the diffraction phenomena which we consider to be the most consistent with reality. This derivation of a mathematical model according to our assumptions and developing algorithms for their solution was a challenging task. This

work has been published in The Journal of MacroTrends in Technology and Innovation, Volume 2 Issue 1, 2014, Monaco, Monte-Carlo [Author related publication 2].

3.1 Introduction

Ultrasound computed tomography in diffraction mode is a technique for tomographic imaging with object of interest in which parameter, such as pressure, sound velocity, etc., can be mapped from scatter wave resulting from the object due to transmission of ultrasound. This kind of mode is sometimes simply called as ultrasound diffraction tomography or just diffraction mode tomography. Diffraction tomography is similar to reflection tomography where instead of summing all the received signals, each one separately recorded and reconstructed taking the Fourier transform of each received signal with respect to time. Diffraction mode tomography uses an approach known as inverse scattering problem for reconstructing the parameters of interest. The direct scattering theory and inverse scattering theory fall under scattering problem theory. The direct scattering theory is to determine the relation between input and output waves based on the known details about the scattering target. The inverse scattering theory is to determine properties of the target based on the computed input-output pairs. Tomographic reconstruction in diffraction mode uses inverse scattering approach also known as forward scattering problem.

Few of the tomographic approaches tried to address inverse problems of ultrasound tomography in terms ray optical models. But as already mention earlier ultrasound modeled as ray essentially may not provide with sufficient information due to physical phenomena associated with the wave nature are not take into account. We address problems of ultrasound tomography in terms of mathematical wave models

describing phenomena such as diffraction, which we consider to be the most consistent with reality. Iwata and Nagata [33] were first to bring in the idea of ultrasonic tomography where they calculated refractive index distribution of object of interest using the Born and Rytov's approximation. In 1974, R.K. Mueller et al. solved for ultrasonic velocity distribution based on wave equation and presented a three dimensional reconstruction of objects from two dimensional profiles in frequency domains. Later, Stenger et al. investigated on this method through various reconstruction algorithms [34] [35].

Diffraction mode tomography can be modelled using single or array of transducers or either using any of the architectures arrangement described in chapter 2 (Figure 9: Different Transducer Arrangements). The figure (Figure 15) below is the basic block diagram of the ultrasound diffraction image acquisition system with ring shaped architecture. The ultrasound pulse generator is used for triggering the transducers for transmitting the ultrasound through the object via a coupling medium. The received data is sent to the electronic processor for conversion, amplification, storage and display. The computation, display and processing is controlled by a computer.

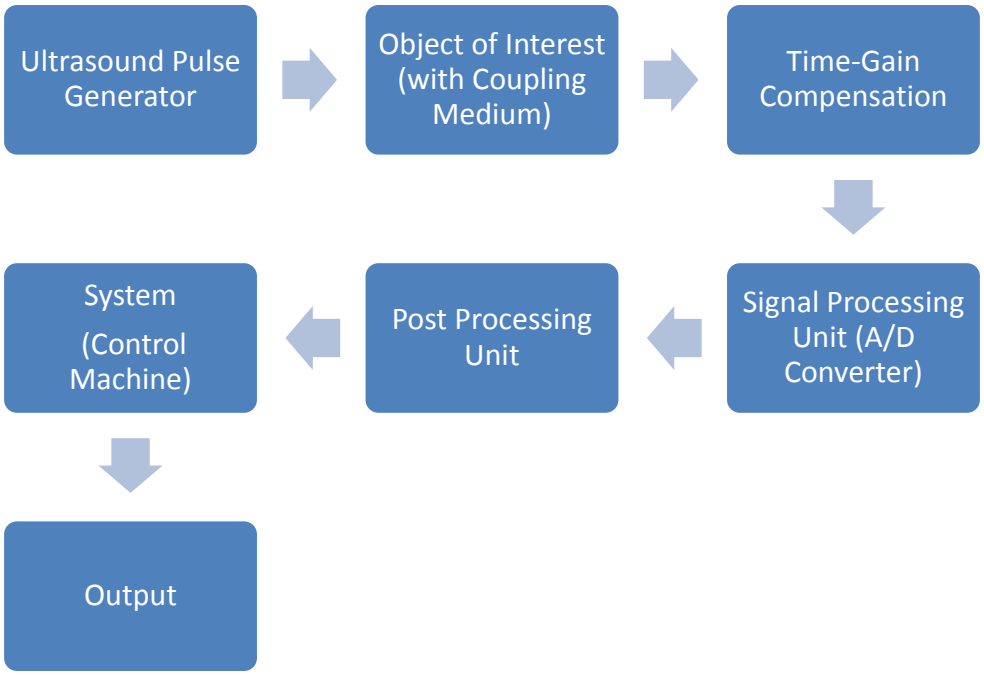

Figure 15: Block Diagram of the Ultrasound Diffraction Image Acquisition System

Based on the state of art, there were two main approaches to solve inverse problems in terms of mathematical model i.e. wave models. The first approach is based on the use of Green's functions considering various linear approximations to the nonlinear problem of ultrasound diffraction tomography, commonly scattering problem is solved with Lippmann-Schwinger or Integral equation using Green's function. But the solution is ill-posed and its validity restricts strongly on the potential of linear approximations. Methods of solution of linear and nonlinear inverse problems represented by operator equations are well known and efficient procedures have been developed to solve them [15, 16]. The other way to solve inverse problems is considering coefficient inverse problems for hyperbolic partial differential equations. It was shown in the nonlinear formulation that gradient-based iterative algorithms for the construction of an approximate solution can be built directly by minimizing the residual functional. This

method to solve inverse problem for ultrasound tomography is without invoking integral representations involving the Green's function [24-27]

The mathematical model established in this chapter uses first approach and it also obtained a number of successful results concerning the solution of inverse problems of ultrasound tomography [31]. Many authors have mathematically well established a wave equation describing the tissue-ultrasound interaction and scattering of ultrasound in the in homogeneous medium. Chernov derived the wave equation in a homogeneous and non-homogeneous medium considering the scattering of ultrasound is due to change in velocity and temperature [53]. Gore and Leeman [57] derived wave equation considered the scattering term as a function of density, Fatemi and Kak [58] described the origination of scattering is due to velocity fluctuation. Similarly Jensen et al [61] established of wave equation in inhomogeneous medium with scattering coefficient in terms of density and velocity.

We consider the scattering of ultrasound in an in homogeneous medium is due to change in compressibility and density. Hence we derive a wave equation, considering scattering term as function of compressibility and density and established a mathematical model supporting this phenomenon. The present work is limited to two dimensional wave model formulated under the assumptions of the Born approximation. Sources and receivers are arranged in a linear or ring shaped array surrounding the object of interest (scattering region).Using Hankel function, the 2D Green's function can be solved for scattered and total pressure fields. The result of experiment investigation of diffraction tomography is very promising.

3.2 Wave Equation Derivation

Consider an object with density ρ_o is insonified by ultrasound wave in the Cartesian coordinates, and then the reconstruction is mapped by solving the forward scattering problem with the linear approximation. Let us assume, the spatial gradient of sound pressure wave in Cartesian coordinates represented as $\nabla p(r,t)$ in the point *r* in the space with *u(r,t)* is the velocity vector of the particle, then according to Euler's equation

$$\rho_o \frac{\partial u(r,t)}{\partial t} = -\nabla p(r,t) \qquad \textit{(eq3.1)}$$

The homogeneous acoustic wave equation can be written as [53];

$$\nabla^2 p(r,t) - \frac{1}{c^2}\frac{\partial^2 p(r,t)}{\partial t^2} - = 0 \qquad \textit{(eq3.2)}$$

Where *c* is the speed of sound in the medium. Let $p_1(r,\omega)$ be the Fourier transform (F.T) of the acoustic pressure *p* i.e.;

$$p_1(r,w) = p_1(x,y,z;\, w) \overset{F.T}{\leftrightarrow} p(x,y,z;t) = \int_{-\infty}^{\infty} p(x,y,z;t) e^{-j\omega t}\, \mathrm{dt}$$

Applying Fourier transforms to the equation *eq3.2* by multiplying by $e^{-j\omega t}dt$ and integrating over $-\infty \; to \; +\infty$ we get Helmholtz equation that can be written as;

$$\nabla^2 p_1(r,\, w) + k^2 p_1(r,\, w) = 0 \qquad \textit{(eq3.3)}$$

where *k* is the acoustic wave number such that $k=w/c= 2\pi/\lambda$. On employing Green's theorem for bounded space of medium of surface *s* and volume *v,* equation *eq3.3* reduces to,

$$\int_s \left(p'_1 \frac{\partial p_1}{\partial n} - p_1 \frac{\partial p'_1}{\partial n}\right) ds = 0 \qquad \textit{(eq3.4)}$$

p'_1 and p_1 may be the solutions of the Helmholtz equation i.e. for a free field, the Green's function is represented as;

$$\nabla^2 g_w(r|r') + k^2 g_w(r|r') = -\delta(r-r') \qquad (eq3.5)$$

Where r' is the position of the point source (for instance, transducer) and $\delta(r-r')$ is the 3D dirac delta function and $g_w(r|r') = \frac{e^{ik||r-r'||}}{4\pi||r-r'||}$. Then the solution to the Helmholtz equation is calculated by [60],

$$G_w(r|r') = g_w(r|r') + X_w(r) \qquad (eq3.6)$$

But practically a human body is an inhomogeneous medium. As discussed earlier when ultrasound penetrates through human body it scatters. Let the scattering term be $f(r,t)$ due to the scattering object at point r' at time t' be a function of compressibility (k) and density(ρ). The wave equation for homogeneous can be rewritten with a introduced scattering term as,

$$\nabla^2 p(r,t) - \frac{1}{c2}\frac{\partial 2\, p(r,t)}{\partial t2} = -f(r',t') \qquad (eq3.7)$$

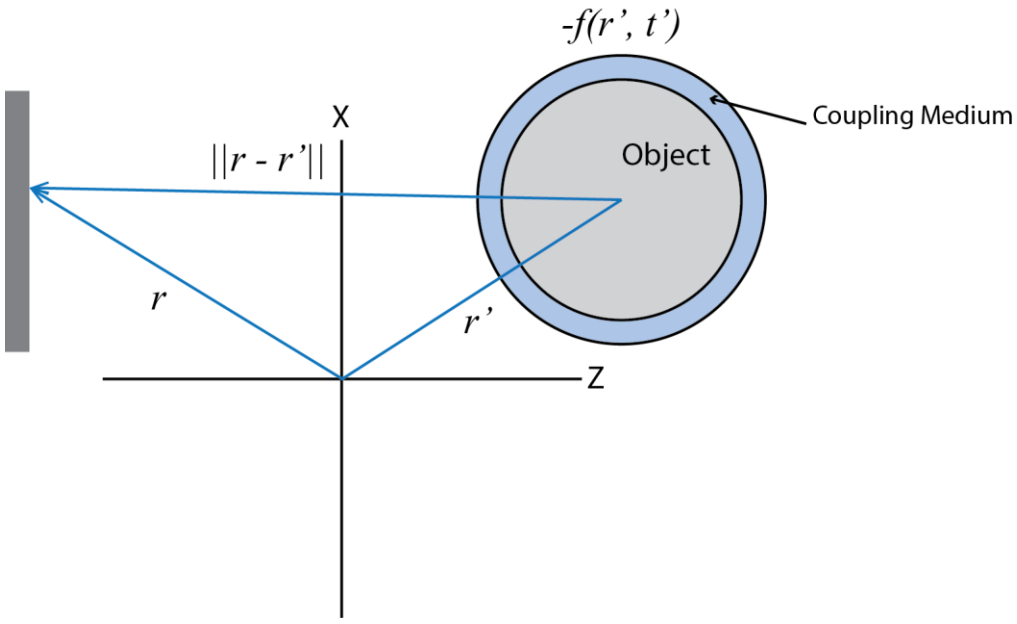

Figure 16: Coordinates System for Scattered Field

We assume the scattering is due to change in density and compressibility of the medium. Wave equation for inhomogeneous medium with scattering field in terms of density and compressibility was derived and represented as [60]

$$\nabla^2 p(r,t) - \frac{1}{c2}\frac{\partial 2\, p(r,t)}{\partial t2} = -\frac{1}{c2}\gamma(r)\frac{\partial 2\, p(r,t)}{\partial t2} + \nabla(\Delta\rho).\nabla P \qquad \textit{(eq3.8)}$$

$\gamma(r)$ is the change in compressibility and $\Delta\rho$ change in density. Using first-order Born approximation, the scattered signal is calculated employing Green's function *g(t)* for unbounded space which is,

$$g(r, t|\, r', t') = \frac{1}{4\pi|r-r'|}\,\delta\left(t-t'-\frac{|r-r'|}{c}\right) \qquad \textit{(eq3.9)}$$

The pressure field in the point r' in the space is calculated as,

$$p(r,t) = \int_V \int_t f(r',t') * g(r,t|\, r',t')\, dv\, dt \qquad \textit{(eq3.10)}$$

From *(eq3.8)* and (*eq3.10)* the measured scattered pressure field p_s (r, t) can be calculated as

$$p_s(r,t) = \int_V \int_t -\frac{1}{c2}\gamma(r)\frac{\partial 2\, p(r,t)}{\partial t2} + \nabla(\Delta\rho).\nabla P * g(r,t|\, r',t')\, dv\, dt \qquad \textit{(eq3.11)}$$

The above equation clearly indicates that for calculating scattered pressure field, we require the incident pressure field i.e. $p(r,t)$. In our study, the incident field is generated by ultrasound transducers which is calculated from solving the wave equation for homogeneous medium by employing a term velocity potential ψ(r, t)

$$\nabla^2\psi - \frac{1}{c^2}\frac{\partial^2\psi(r,t)}{\partial t^2} = 0 \qquad \textit{(eq3.12)}$$

And pressure field is calculated as;

$$P_i(r,t) = \rho_0 \frac{\partial\, \psi(r,t)}{\partial t} \qquad \textit{(eq3.13)}$$

$$= \rho_0\, v(t) *_t \frac{\partial h(r,t)}{\partial t} \quad or$$

$$=\rho_0 \frac{\partial v(t)}{\partial t} *_t h(r,t) \quad \textit{(eq3.14)}$$

h(r,t) is the spatial impulse response of the transducer and v(t) is the transducer's velocity which includes electromechanical impulse response $\xi_m(t)$ of the transducer but we neglect this term in our case.

3.3 Spatial Impulse Response

There are numerous ways proposed by various authors for calculation of spatial impulse response for ultrasonic field for different apodization [21] [59]. Spatial impulse response indeed is the output received i.e. behavioral change with impulse signal as input. A linear system Ș responds to input impulse signal δ(x, y), then the output of the system is determined by impulse response h(x, y) such that,

$$h(x, y)=Ș[\delta(x, y)] \quad \textit{(eq3.15)}$$

Assume f(r) is the input for the linear system Ș and g(r) is the output which is given as

$$g(r)= h(r) * f(r) \quad \textit{(eq3.16)}$$

The transfer function of the system is the Fourier transform of the impulse response.

Now let as assume in our case that the system is linear and shift invariant. The transducer is fixed at point *r* and it transmits ultrasound waves through the object wit density *ρ* and the scattered field is located at *r*'. Huygen's principle assimilates each point of a radiating surface as the origin of an outgoing spherical wave. An excitation of the transducer with an impulse function δ (t) will give rise to a pressure field. Let the distance between transducer and scattered field $(r' - r)$ be *d* and spatial impulse response *h(r,t)* for ultrasonic pressure fields along the integration of the surface s can be calculated as;

$$h(r',t)= \int_s \frac{\delta(t-\frac{|r'-r|}{c}}{2\pi|r'-r|} ds \quad \textit{(eq3.17)}$$

The Figure 17 shows the flow chart for computation of spatial impulse response used in our case.

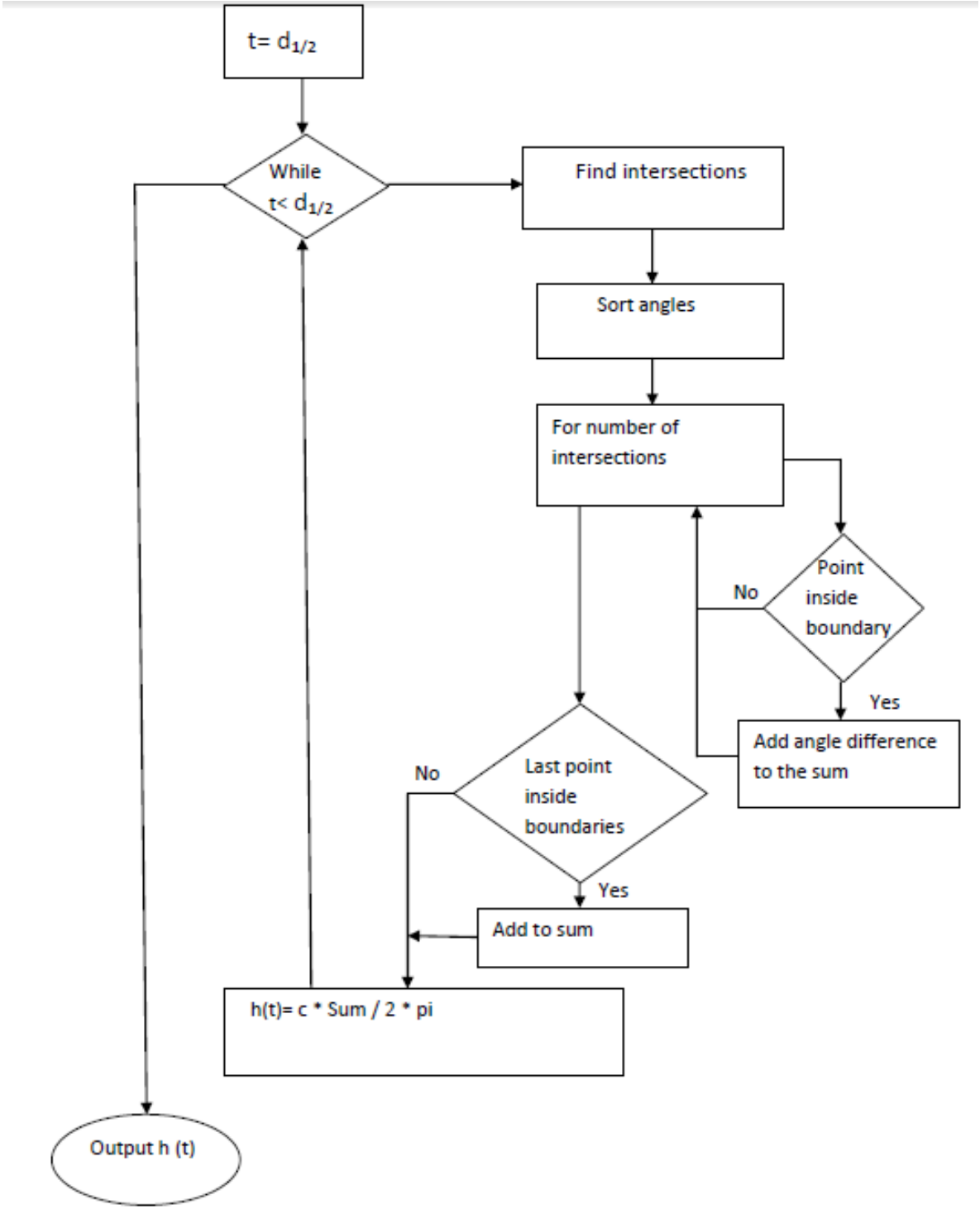

Figure 17: Flow Chart for Computation for Spatial Impulse Response

The total received field over the transducer can be represented as $p_r(r,t)$, represented as;

$$p_r(r,t)= \xi_m(t) * \int_s p_s(r,t)d^2r \qquad (eq3.18)$$

Assuming electromagnetic impulse response (which can be calculated manually) is neglected, and then the received field is the integration of the collected scattered field over the transducer surface. The characteristic of the scattering field determines the tissue property. Hence this scattering field forms the base of the ultrasound computed tomography in diffraction mode.

3.4 Simulation of Wave Equation

The measured scattered field is represented as, from equation *eq3.11,*

$$p_s(r,t) = \int_V \int_t - \frac{1}{c2}\gamma(r)\frac{\partial 2\, p(r,t)}{\partial t2} + \nabla(\Delta\rho).\nabla P * g\,(r,t|\,r',t')dv\,dt$$

For a computer simulation the scattered pressure field $p_s(r)$ in the region interest is digitized into NxN square pixels when applied by an incident pressure field $p_i(r)$ is given as,

$$p_s(r)=p(r)- p_i(r) \qquad (eq3.19)$$

Now we know using Born's approximation, the scattered field is solved. Then solution would be,

$$p_s(r)=\iint o(r)\, p_i(r)\, g(r,t|r',t')\, dv\, dt \qquad (eq3.20)$$

where $o(r)$ represents the scattering term. General expression for the scattered field is

$$p_s(r,t)= g_i\, o(r)\, p_i(r',t)+ [g_i\, o(r)]^2\, p_i(r',t) + [g_i\, o(r)]^3\, p_i(r',t) +\ldots \quad \text{(For i=1 to N)}$$

Considering for a delta function as the test function, the measured field at any point in the medium is,

$$p_s(r)=\sum_j o(r)\, p_i(r) \int g(r,t|r',t')\ \delta(r-r')dr'dt \qquad j=1,2,3\ldots N$$

So, $p_s(r) = \sum_j o(r)\, p_i(r) \int g(r, t|r', t')\ dr'$ *(eq3.21)*

Using Hankel function, the 2D Green's function can be solved. According to Hankel function properties, we know that for scattering point source *r'* of radius *a* and distance (*R*) between *r* and *r';*

$$\int g(r, t|r', t')\ dr' = \begin{cases} \frac{j}{2}\ [\pi k a H^2(ka - 2j)] & for\ i = j \\ \frac{j\pi ka}{2}\ J(ka)H^2(kR) & for\ i \neq j \end{cases} \quad \textit{(eq3.22)}$$

K is the wave number, J is the first kind of Bessel function and *H* is the second class of first order Bessel function. On applying *(eq3.21)* on *(eq3.22),* the receiving scattering field due to scattering point source r' can be transformed into,

$p_s(r) = \sum_j o(r)\, p_i(r)\, d_j$ where $d_j = \frac{j\pi ka}{2}\ J(ka)H^2(kR)$ *(eq3.23)*

The total pressure field can be calculated as,

$p(r) = p_i(r) + \sum_j o(r)\, p_i(r)\, d_j$ *(eq3.24)*

The pressure field can be simulated using equation above. The input would be a plane ultrasound wave which transmits through the body and a scattered field is displayed at the output. Figure 18 below shows a sample scattered pressure field output in amplitude spectrum for a plane ultrasound wave of 2 MHz encountering a muscle with bone at the center.

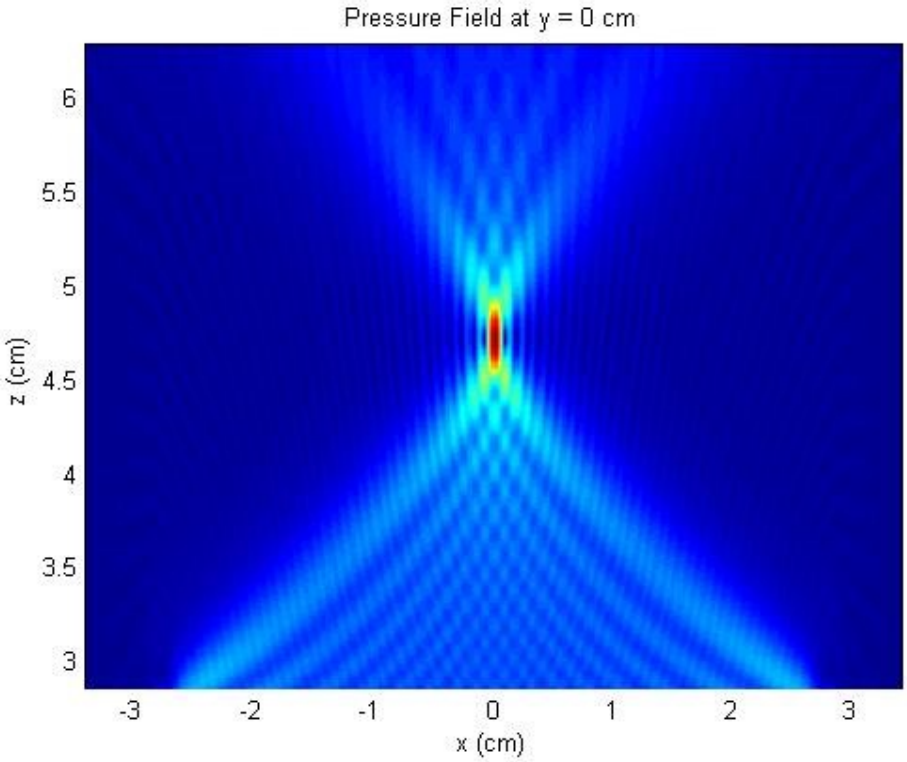

Figure 18: Simulated Scattered Pressure Field Plotted for Muscle

4 Chapter: Diffraction Mode Tomogrpahy Reconstruction

In the previous chapter, we have formulated a mathematical model to describe the ultrasound wave propagation through a non-homogeneous medium. We have found the scattering coefficient terms produced due to transmission of ultrasound through tissues. This coefficient alone cannot describe the tissue property nor it be analyzed by a physician. Hence, the process of extracting the image from the obtained parameters is called reconstruction. The measurements made in Ultrasound computed tomography in diffraction mode can be sampled using simple radon transform of the distribution of refractive index in the slice being imaged. The radon transform and its inverse of provide the basis for reconstruction of images. There are many different reconstruction approaches such Fourier slice theorem, Filter back projection, etc. discussed in chapter 2. These approaches assume the ultrasound wave propagation as straight line which is not likely in our case. These straight ray tomographic reconstruction approaches are no longer applicable while considering diffractive sources. Many authors have discussed various approaches to reconstruct images from a diffraction tomography but these methods are computational either expensive or complex. In this chapter, we propose a new method of reconstruction in ultrasound computed tomogrpahy in diffraction mode.

4.1 Fourier diffraction theorem

Assume an object $f(x)$ to be imaged coupled with water is insonified by a monochromatic plane ultrasound wave (Figure 19) with wave number $K=2\pi/\lambda$ and frequency $\omega=2\pi c/\lambda$ through a transducer placed such that the projection angle θ with z axis , then the total pressure is calculated as;

$$p(r)= p_s(r)+p_i(r) \qquad (eq4.1)$$

such that p_i and p_s are the incident pressure field and is the scattered pressure respectively. On solving wave equation in nonhomogeneous medium the incident pressure field and scattered pressure field are determined as;

$p_i = \rho_0 \frac{\partial v(t)}{\partial t} *_t h(r,t)$ *and* *(eq5.2)*

$p_s(r) = \iint o(r)\, p_i(r)\, g(r,t|r',t')\, dv\, dt$ *(eq4.3)*

where $o(r)$ represents the scattering term of the object with density ρ_0 and *h(r,t)* is the spatial impulse response of the transducer and v(t) is the transducer's velocity. The ultimate goal is to reconstruct the obtained resultant data into an informative and original desired object to be imaged. This can be achieved by applying Fourier transform to the measured scattered field projection on the object.

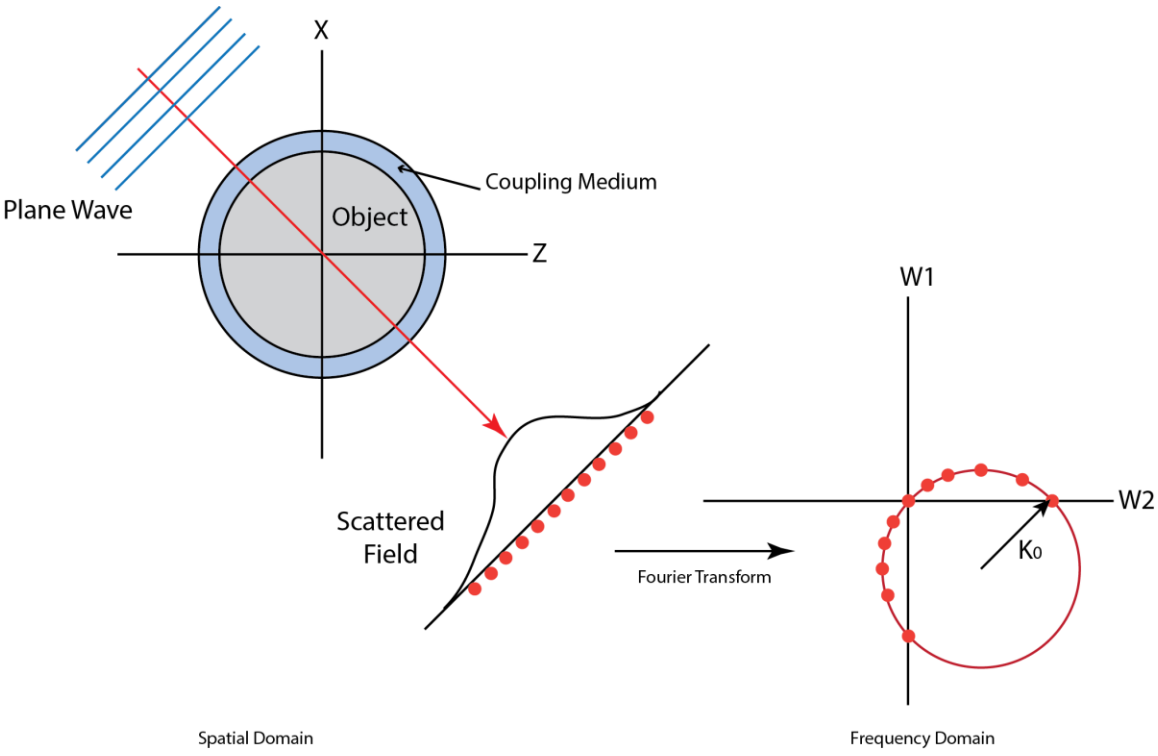

Figure 19: Illustration of Diffraction Mode Tomography

The projection data $P_\theta(r)$ obtained from θ= 0 to 2π yields the Fourier transform of the scattered field $p_s(r)$ in spatial frequency domain such that;

$F\{P_\theta(r)\}(\omega) = F_{2D}\{f(x)\}\{w_1, w_2\}$ where F and F_{2D} are the 1-D and 2-D Fourier transforms respectively and

$$w_1(r) = \omega \cos\theta - (\sqrt{k_0^2 - \omega^2} - k_0) \sin\theta, \quad (eq4.4)$$

$$w_2(r) = \omega \sin\theta + (\sqrt{k_0^2 - \omega^2} - k_0) \cos\theta \quad (eq4.5)$$

The Fourier transform of the scattered field ps(r) measured along the projected line l with angle θ

$$p_s(k, \theta) = \int_{-\infty}^{\infty} ps(r) e^{-jkl} dl \quad (eq4.6)$$

is given by

$$P_s(k, \theta) = \frac{k_0^2 p_0}{j2\gamma} e^{j\gamma O(k)} \quad (eq4.7)$$

$\gamma(r)$ is the change in compressibility. The Fourier transform of the scattered field gives the values of arc as shown in Figure 19. That is the Fourier transform of object (scattering term) along the semi-circle of radius $k_0 = 2\pi/\lambda$ *is*

$$O(k, \theta) = \frac{j2\gamma}{k_0^2 p_0} e^{j\gamma Ps(k,\theta)} \quad (eq4.8)$$

The above equation is the Fourier diffraction projection theorem, which related the Object (scattering term) and the scattering field.

The transmitted wave is a superposition of monochromatic waves at different frequencies forming a broad band illumination. This is an advantage because more information is obtained from a single projection than in straight ray tomography because the frequency domain is sampled on several arcs simultaneously. Consequently, a smaller amount of projections should suffice for covering the entire frequency domain. The

Figure 20 below represents the broad band illumination of 6 arcs and 4 projections with 32 sampling points.

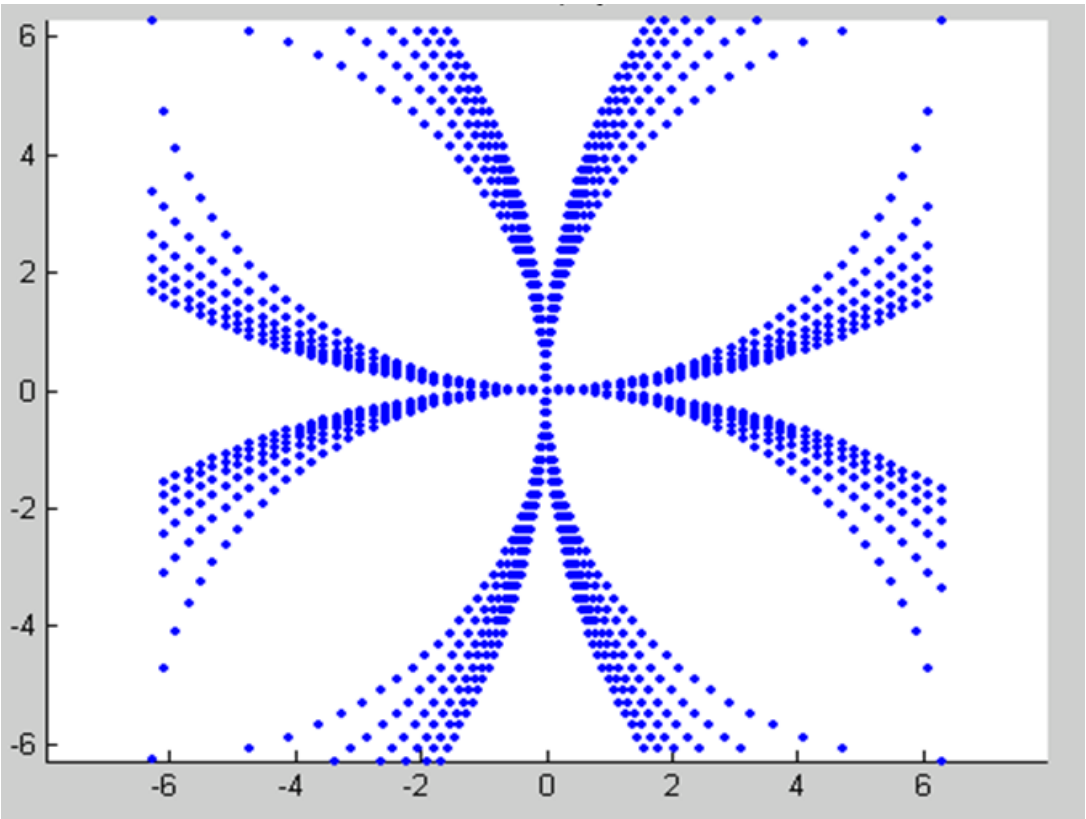

Figure 20: Sampling Corresponding to 6 Broad-Band Projections

Direct calculation of the Fourier diffraction theorem given by

$$f_j = O(k, \theta) = \sum_{k=-N/2}^{\frac{N}{2}-1} \frac{j2\gamma}{k_0^2 p_0} e^{j\gamma Ps(k,\theta)} \text{ for } j = -N/2, \ldots N/2-1 \qquad (eq4.9)$$

requires N^2 arithmetic operations. The inversion of Fourier diffraction theorem can reconstruct the image back. This reconstruction of image from the established set of sample data can be done by using simple inverse Fourier transform with complexity [O $(N)^3$]. This is a direct approach for reconstruction. It might be easier to look but it has very slow convergence rate, especially for non-homogeneous medium. This is one of the

major drawbacks for reconstruction of diffraction tomography i.e. high complexity during reconstruction. This direct approach is very expensive too.

The output received data might be in irregular spacing. Some reconstruction processes work best when the data is evenly sampled in both space and time. This can be achieved by the process of interpolation. The reconstruction approach in diffraction tomography can be categorized into two divisions based on;

- Interpolation in spatial domain
- Interpolation in frequency domain

4.2 Interpolation in Spatial Domain (Filtered Back-Propagation Method)

Interpolation spatially in much the same we as we resample data in the time domain. In spatial domain, linear interpolation for simple first degree interpolation is equivalent to convolution of the input image f(x) with the following kernel function:

$$h(x)=\begin{cases}1-|x| & |x|<1\\ 0 & Otherwise\end{cases} \qquad \textit{(eq4.10)}$$

The unknown parameter *a* can vary between -3 and 0. Based on image content, the values for the parameter *'a'* are decided. For instance, if the goal is to enhance edges suitable values for '*a'* would be $a = -0.75$ or $a = -1$. A Classic example of interpolation in spatial domain was back-propagation approach by Devaney [36]. He tried to investigate that filtered back projection reconstruction approach is not suitable for diffraction tomography. He proposed propagation-back propagation method, which explains the propagation of ultrasound waves through tissues and back propagation for reconstruction using a low pass filter. This filtered back propagation method was followed the filtered back projection principles with few modification to suit for diffractive source and yielded

images with high resolution. He defined the back propagation for a scattering term O(r) at position r' due to transmitted wave along a line with angle θ and tangent to a circle centered at r and with radius l in two operational ways; the first way is at fixed angles *(eq4.11.1)* and the other way was interpolation over different angles *(eq4.11.2)* respectively;

$$\pi_{\phi 0}(r') = \int_{-\infty}^{\infty} H_{\phi}(r') G(r', r' - l)\, dr' \qquad (eq4.11.1)$$

$$O(r) = 1/2\pi \int_{-\pi}^{\pi} \prod_{\theta}(x sin\theta - y cos\theta)\ (; x cos\theta + y sin\theta)\, d\theta \qquad (eq4.11.2)$$

H_{ϕ} is the back propagation filtering coefficient and G(r) is the green's function. This kind of method is computationally extensive and complex. Researcher found that bilinear interpolations followed by 2D inversion have yielded better results than filter back propagation methods [52]. The other kind of approach, the interpolation in frequency domain is much efficient and less complex.

4.3 Interpolation in Frequency Domain

The objective of interpolation in frequency domain is to reconstruct the object function from direct 2D inversion of the frequency domain information. Interpolation gives the approximating function that is constructed to match the values of the discrete function i.e. samples over the arc AOB generated by diffraction tomography (Figure 21). To achieve this we must set few uniform parameters for representing arc grids and the rectangular grids suitable for image reconstruction. The Fourier transform of scattering field and scattering object on the arc AOB was given by (*eq4.7*) and (*eq4.8*)

Let the parameters representing each point on the arc AOB be (k, θ) and the rectangular coordinates in the frequency domain will be denoted by (w_1, w_2).

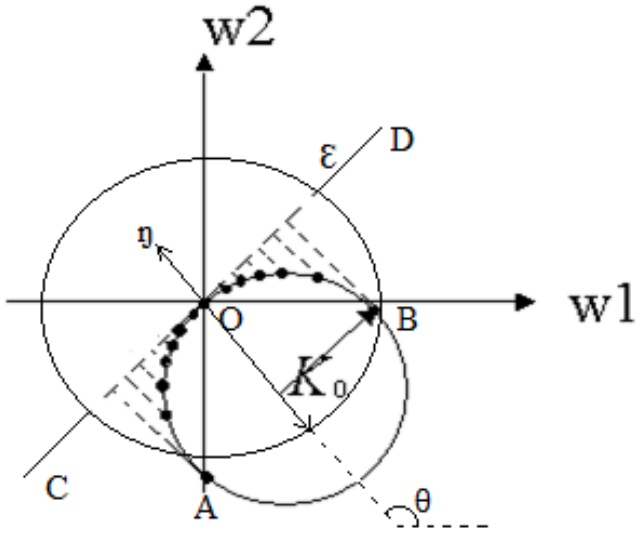

Figure 21: Samples over the Arc AOB Generated by Diffraction Tomography

Let the polar coordinates of (w_1, w_2) be expressed as (W, ϕ) as;

$$W=\sqrt{w_1^2 + w_2^2} \text{ and } \phi= \arctan\left(\frac{w_1}{w_2}\right) \qquad \text{(eq4.12)}$$

It is clearly seen the arc AOB generates a double coverage of the frequency domain (Arc AO and OB), hence it is appropriate to consider separately the points generated by the arc AO and OB as shown in the Figure 21 and the arc grid can be represented as (k_1 , θ_1) and (k_2 , θ_2) for arc AO and OB respectively from [52]

$$k_1 = \sin(2 \arcsin(W/2 k_0)), \qquad \text{(eq4.13.1)}$$

$$\theta_1 = \arctan(w_1 / w_2) - \arcsin(W/2 k_0) + \pi/2 \quad \text{and}$$

$$k_2 = -\sin(2 \arcsin(W/2 k_0)), \qquad \text{(eq4.13.1)}$$

$$\theta_2 = \arctan(w_1 / w_2) - \arcsin(W/2 k_0) + 3\pi/2$$

The reconstruction technique using interpolation can be defined as;

$O(k, \theta) = \sum_{i=1}^{n} \sum_{j=0}^{m} O(k_i, \theta_j) H_{i,a}(k) H_{i,a}(\theta)$ *(eq4.14)*

Where H is the kernel function in frequency domain of order a, such that a=2 for bilinear interpolation and $H_{i,a}$ for bilinear interpolation can be given as;

$$H_{0,2} = \begin{cases} |x| & for\ 0 \le |x| < 1 \\ 2 - |x| & for\ 1 \le |x| < 2 \\ 0 & Otherwise \end{cases} \quad (eq4.15)$$

The complexity for bilinear interpolation can be calculated as O ($4N^2+N^2$ log (N^2). This is also called as Gridding algorithm.

4.4 Reconstruction Approach

Due to high complexity and long computation time of direct reconstruction approach we propose an iterative reconstruction for ultrasound computed tomography in diffraction mode which reconstructs the images in a non-homogenous medium. This approach is also known as iterative reconstruction for Non-uniform Fourier transform (NUFT). This is a fast method for DFT proposed by Cooley and Tukey (1965). The improvise version of NUFT is by introducing fast Fourier technique, hence named as Non-uniform fast Fourier transform (NUFFT). This is an Iterative reconstruction method which reconstructs the object functions from non-uniform samples of the frequency domain information without using the gridding algorithm. Assume an object of interest is targeted with ultrasound plane wave, which is transmitted through a coupling medium and received in output as a scattering field due to scattering term. The object of interest can be reconstructed back from the obtained Fourier diffraction coefficient (*eq4.8*) using Non-uniform Fourier transform defined as;

$f_j = O(k, \theta) = \sum_{k=-N/2}^{\frac{N}{2}-1} f_n\, e^{jt\gamma\theta}$ *for j= -N/2,....N/2-1* *(eq4.16)*

such that θ = { $\theta_{-N/2}$, …. $\theta_{-N/2-1}$} belongs to [0,2π] be the vectors of non-uniformly distributed scattering term along the arc over the time t= { $t_{-N/2}$, …. $t_{-N/2-1}$} and $f_n = \frac{j2\gamma}{k_0^2 p_0}$.

This *(eq5.16)* can be rewritten in matrix form as;

$$f_j = F(f_n)_j \qquad (eq4.17)$$

The equation can be bounded and reduced on introducing a finite sequence term S(j) defined as;

$$S(j) = s_j e^{-i2\pi tj/N} \equiv s_j Z^{imt} \text{ for } j = -N/2, \ldots N/2-1 \qquad (eq4.18)$$

Where the accuracy factors $0 < s_j < 1$ are chosen to minimize the approximation error. Least square interpolation of $p_s(\theta)$ of finite sequence term along the arc AOB is given as;

$$s_j Z^{imt} = \sum_{\theta=0}^{2\pi} ps(\theta) Z^{j([mt]+\theta)} \qquad (eq4.19)$$

The simplified least square solution can be written as ;

$$ps(\theta) = F^{-1} a(\theta) \qquad (eq4.20)$$

The matrix $F = A^t A$ where $A = Z^{j([mt]+\theta)}$, hence the matrix F=

$$\begin{bmatrix} N & \cdots & \frac{Z^{-qN/2} - Z^{qN/2}}{1 - Z^{-q}} \\ \vdots & \ddots & \vdots \\ \frac{Z^{N/2} - Z^{-N/2}}{1 - Z^{-1}} & \cdots & N \end{bmatrix}$$

Here the parameter '*a*' is unknown and could be calculated as using different accuracy factors. In our case we use Gaussian accuracy factor given by

$$s_{j=} e^{-b(\frac{2\pi j}{Nm})^2} \text{ and } a(\theta) = \sum_{j=-N/2}^{\frac{N}{2}-1} sj e^{i\frac{2\pi}{Nm}([mt]-\theta)j} \qquad (eq4.21)$$

The basic NUFFT algorithm steps are

(i) Initialization all the parameters and sampling ratio

(ii) Computation of scattering terms and Convolution for each source point.

(iii)Fast Fourier transforms

(iv)Inverse convolution

The toughest task in NUFFT calculation is computing the scattering term because it is an ill-posed problem. (In the following chapter we would discuss further about ill-posed problem.) In practice 'd' dimension, the process requires 12^d N exponential evaluations for single precision which could further become a burden for higher dimensions and with higher precision accuracy. This would increase the storage space and computation time. Therefore to solve this ill-posed problem and decrease the computation time, we introduce an additional regularization term during convolution which prevents it from over fitting or unnecessary iteration, yet preserving the accuracy.

4.5 Regularization

The best reconstruction method gives the best replica of the measured object. As we already know Diffraction mode tomography uses an approach known as inverse problem for reconstructing the parameters of interest. The inverse scattering problem which is established based on wave theory can be ill posed equation. Reconstruction of the image from the above formulated equation can be very time consuming because it has no proper converging point. Introducing of a regularization term is a method to solve these ill-posed problems. Inverse problem is a method of determining the cause for a desired or an observed effect. Usually when the details about the scattering target i.e. the cause is already know, the effect i.e. the output is determined by direct problem approach. Figure 21 relates the direct problem and inverse problem between input and output waves.

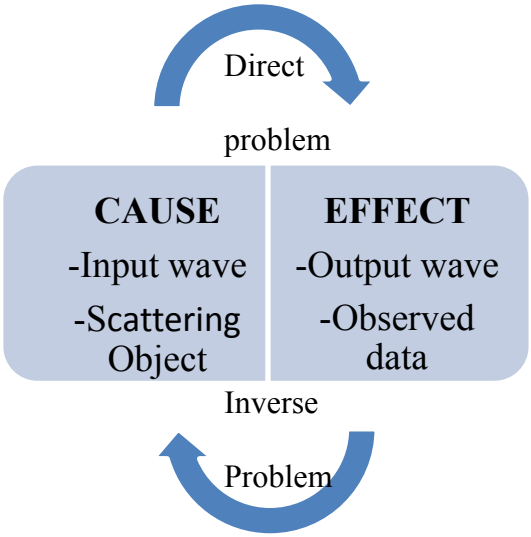

Figure 22: Direct Problem and Inverse Problem

Consider an Linear shift invariant system (LSI-Figure 23) with input f(t) and the received or observed output is g(t).

Figure 23: A LSI System

The output g(t) can be determined by direct problem method, such that,

g(t)= f(t)*h(t)

$$=\int f(t')h(t-t')dt' \qquad (eq4.22)$$

In Fourier domain, the solution is

g(ω)= f(ω) h(ω) and

$$h(\omega)=\frac{1}{1+j\omega r} \qquad (eq4.23)$$

The solution for such direct problem approach would be stable i.e. well posed and the observed output would be a closed set. According to Hadamard, 1923 direct problem approach is well posed because of its existence and uniqueness of solution and its continuous dependence of solution on the data .Inverse problem is the vice versa of the direct problem because here we try to determine the unknown parameter of object from the observed data. In such case we determine *f(t)* i.e. the original input from the received data g(t). Consider A is an operator of the LSI system such that output is determined by,

$$g(t)=A\,f(t) \qquad (eq4.24)$$

Therefore a generalized solution would be,

$$f(t)= A^{-1}\, g(t) \qquad (eq4.25)$$

In Fourier domain it can be represented as,

$$f(\omega)= \; g(\omega)\,(1+j\omega r) \text{ and} \qquad (eq4.26)$$

$$h' is\ unbounded \begin{cases} |h'(\omega)| \to \infty \\ \omega \to \infty \end{cases}$$

Practically, the observed data might not be the replica of the original image due to random added noise or artefacts such that output $g(t)_\sigma$ with the noise is given as;

$$\Delta g(t)_\sigma = A\,\Delta f(t) + \sigma \qquad (eq4.27)$$

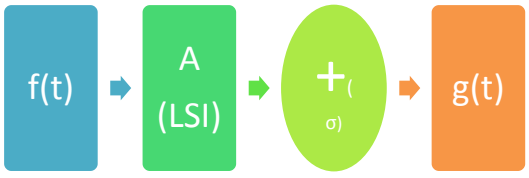

Figure 24: A LSI System with Noise

A perturbation Δg' on g' leads to a perturbation on f' given by

$$\Delta f'(\omega) = \Delta g'(\omega)(\,1 + \,j\omega r) \qquad (eq4.28)$$

The size of noise $\sigma = \| A(\Delta f(t)^t) - \Delta g(t)_\sigma \|$

According to Hadamard the solution of inverse problem is well-posed if a solution exists for any g(t) in the observed data space and is unique and also the inverse mapping of g(t) from f(t) is continuous. Therefore, if the solution of such approach is unstable and it lives in infinite dimensional spaces then the inverse problem is said to be ill-posed. Also if the operator is linear then it's a linear ill-posed problem or if it's non-linear, it is a non-linear inverse ill-posed problem respectively. For instance in linear case, such that A is a linear operator, the inverse problem is said to be well-posed if a solution exists in the observed data space and is unique i.e. Null $(A) \equiv \aleph(A) = \{0\}$ and range$(A) \equiv \sum(A) = y$. If the linear operator is a finite dimensional, then it holds good for both $(A) \equiv \aleph(A) = \{0\}$ and range$(A) \equiv \sum(A) = y$. But for infinite dimensional space, the conditions may not be validated, i.e. a solution may exist but it may not be in the range (A) because it is unbounded. The stability is lacking because of no proper converging point. The ultrasound diffraction is an unbounded property; the formulated wave equation in the previous chapter can be very time consuming because A is a continuous iterative operator and it has no proper converging point. This kind of ill-posed problem can be stabilized using a tight bound condition such as,

$$\frac{||\Delta f||}{||f||} \leq \text{Condition}(A) \frac{||\Delta g||}{||g||} \qquad \textit{(eq4.29)}$$

This condition/ stabilizing term is called regularization operator. This introducing of a regularization term is a method to solve these ill-posed problems. Regularization is a process of introducing additional information in order to solve an ill-posed problem or to prevent over fitting. That is approximating the inverse F by a family of stable/Regularization operator R_α (F^{-1} R_α). R_α is the regularization term with

regularization parameter ‘α’. Choosing of an appropriate regularization parameter α is essential because it trades off between approximation and stability. A small α may define a good regularization approximation for the inverse problem but the solution might be unstable. A large α may give a stable solution but it is a bad approximation for inverse problem. Therefore, choosing perfect and suitable regularization parameter α is very important. The total error is the sum of approximation error and propagated error. The relationship between approximation error and propagated error over the regularization term is depicted in the graph below (Figure 25)

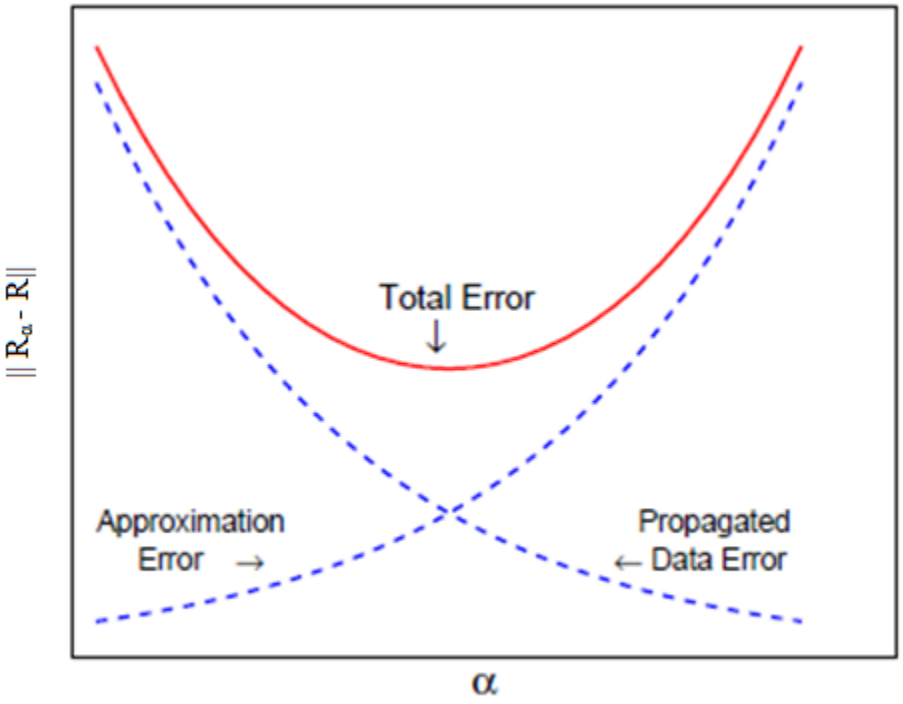

Figure 25: Relationship Between Approximation Error and Propagated Error Over the Regularization Term

This ‘α’ Parameter can be selected in three different ways using the parameters Choice rule defined below;

- a – priori α = α (δ): This is easy to implement but needs info on source condition

- a – posteriori α = α (δ,y): This is also easy to implement and no info on source condition is required but in some cases it is not for optimal order. This is also referred to as raus rule..
- Heuristic α = α (y):This is selected according to Quasi-Optimality rule or Hanke-Raus rule

After choosing the good parameter, we implement the regularization operator for ill-posed inverse problem. Fessler and Sutton obtained such regularization term for interpolation coefficient that minimize the max approximation error at given point of the non-uniform grid over all signals with unit l_2 norm the formulated is min.max problem as

$$min_{u-k}\ max_{||f||\leq 1}\ |\ u_k\ \emptyset_p^k f_j\text{-}\theta_k f_j|^2 \qquad \textit{(eq4.30)}$$

u_k is the non-zero^{th} row of interpolation matrix O_p. The accuracy of algorithm was not tested.

Michael M. Bronstein et al. tried to solve the similar case using total variation regularization given by

$$T_v(\mathrm{f}) = \sum_{i,j} \sqrt{[f(x)]_{ij}^2 + [f(y)]_{ij}^2}$$

And introduce addition penalty for smoothed T_v, which is given as

$$\varphi(x) = \sum_{i,j} \sqrt{[f(x)]_{ij}^2 + [f(y]_{ij}^2 + \eta}$$

They also compared with l_2 and l^θ norm. It required fewer projections for reconstruction but the complexity of arithmetic calculation was same as basic gridding algorithm. The other methodologies stand out good in their own way but are not well suited for diffraction

There are many different regularization methods which can be specifically used for different operation like Truncated SVD, Selective SVD, Total Variation, etc [43] [44]

[45]. One such is the Tikhonov regularization which most popular approaches to solve discrete ill-posed problems. But its applicability on ultrasound diffraction problem was tested using a computer simulation where the scattering term can be estimated using Tikhonov regularization. We test our algorithm with Tikhonov regularization with l_1 norm. This yields better results when compared to other as it saves a lot of time. These results are compared with other reconstruction methods and are mentioned in detailed in simulation and results chapter.

4.5.1 Tikhonov Regularization (TR)

Tikhonov regularization is a widely applied and easily implemented technique for regularizing discrete ill-posed problems. In our case, ultrasound computed tomography in diffraction mode is also an ill-posed problem. On applying the Tikhonov regularization, the series solution has coefficients that are functions of the regularization parameter controlling the degree of regularization. This in turns give greater weight to model elements associated with larger singular values.

Let F(x, y) be non- linear between Hilbert spaces with x, y in operator domain. In the zeroth order Tikhonov regularization, we consider the linear least squares problem solution can adequately fir the data in the $\| F(x) - y\|^2$ such that $\| F(x) - y\|^2 \leq \delta$.

Convergence rates are possible, if x^t in some smoothness class i.e. convergence rate requires a source condition

$$x^t \epsilon M \qquad \textit{(eq4.31)}$$

For, linear ill posed problems in Hilbert spaces, we can form

$$M = x^t = \{ x^t = (F^*F)^{v_w} / w \epsilon x \} \qquad \textit{(eq4.32)}$$

But for Non-linear Case with higher order, we would like to minimize some other measures of M, expressed as R(x), such that the norm of the first or second order derivative of m, gives a preference for a 'flat' or 'smooth' model. Then the solution for regularized least square problem is defined as;

$O(x)= ||F_M -y)||^2 + \alpha R(x)$ *(eq4.33)*

Parameter Choice rules for this approach is 'a –priori with $\alpha=\delta^{\epsilon'}$ or 'a –posteriori with Discrepancy principle. There are various selections of norms such as Sobolev norm i.e. R(x) = $||x||^2 H_s$ or Total Variation i.e. R(x) = $\int |\nabla x|$ or L^1 Norm i.e. R(x) = $\int |x|$ or Maximum Entropy such that R(x) = $\int |x| \log |x|$

We want to limit the convolution for our discretized ill-posed problem. L1 norm is an idle for such situation and would give favorable solutions that are relatively constant (existence).

The above *eq4.33* can be rewritten in matrix form as;

$$\min\left\|\binom{F}{\alpha L}M - \binom{y}{0}\right\|^2 \qquad \textit{(eq4.34)}$$

4.6 Proposed Method

We understand that the dominant task of NUFFT is calculation of Fourier co-efficient. We make certain modifications in NUFFT reconstruction approach for faster calculation of Fourier coefficient for better computation time by adding of an additional coefficient factor, called regularization term to prevent from over fitting. In this proposed reconstruction method interpolation is carried in frequency domain. The results yielded are satisfactory with better computation time and high resolution.

Assume an object to be imaged at position r is targeted by plane ultrasound wave such that it propagates through the object and form a scattering field P_s(r) given by,

$P_s(r) = P(r) - P_i(r)$ *(eq4.35)*

Using Born's approximation and applying Green's function for unbounded space, the scattered field is solved as below,

$$P_s(r) = \iint o(r)P(r)G(r,t|r',t') \quad \textit{(eq4.36)}$$

o(r) is the scattering object. The scattering field is calculated as shown in the algorithm below (Figure 26);

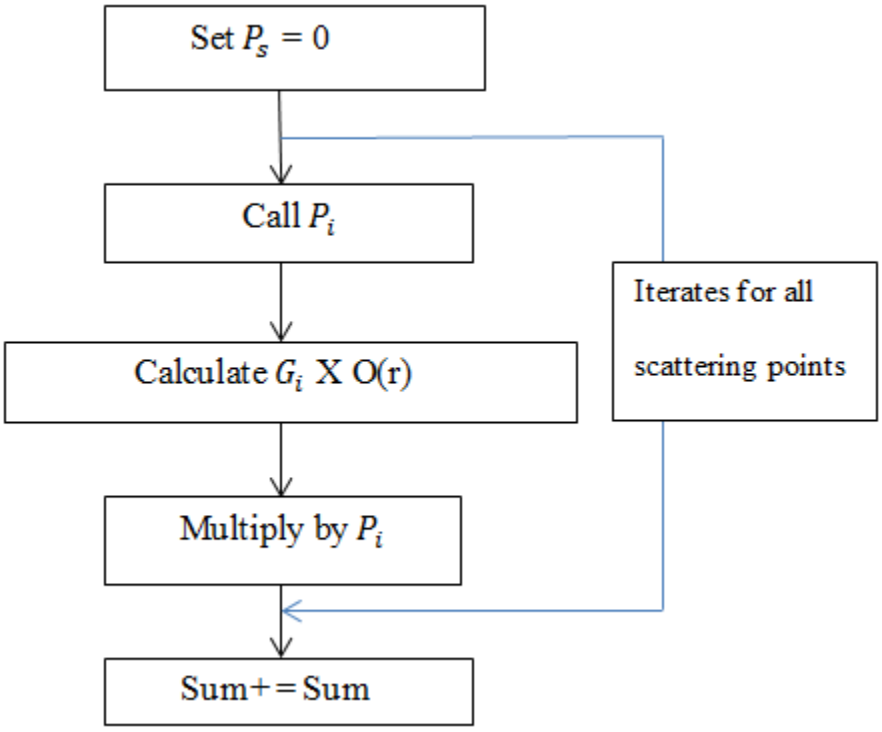

Figure 26: Algorithm for Calculation of Scattered Field

Initially the scattering pressure field P_s is initialized to zero. For every iteration, the incident pressure field is calculated and convoluted with Green's function and discretized scattering coefficient term and adds to the sum every loop. The total sum is the resultant scattered pressure field. Here the region of interest discretized into NxN square pixels is

given and solved by method of moment utilizing and delta functions. The pressure in grid points can be presented in an N2x1 vector as

$$P_s(r) = (D).O.P \qquad (eq4.37)$$

Here P matrix represents initial pressure point, D is the operating matrix and O is the scattering coefficient matrix. If the number of transmitters and receivers are N_t and N_r, respectively, then the scattered pressure can be obtained as,

$$P_s(r) = M.O \qquad (eq4.38)$$

where M= D.P is the matrix whose size is N_t, N_r X N^2

O was updated with every iteration by Tikhonov regularization with l1 regularization norm given by,

$$O=\min\| P_s-MO\|^2 + \alpha\|L_1\|^2 \text{ and} \qquad (eq4.39)$$

$$L_1=\begin{bmatrix} -1 & 1 & -1 & \cdots & & -1 & \\ & \vdots & & \ddots & & \vdots & \\ & 1 & & \cdots & 1 & -1 & 1 \\ & & & & -1 & 1 & -1 \end{bmatrix}$$

Introduction of this regularization term during filtered back projection yield images with high resolution. It also reduces the complexity and decreases the reconstruction time.

5 Chapter: Simulation and Result

Ultrasound computed tomography was undergoing research from past 20 years. Many computer simulations testing these methods have met success but currently, there are no commercially manufactured ultrasound computed tomography's for whole body scanning for clinical applications due to high complex computation time for reconstruction or big data problem. Most of these ultrasound computed tomography approach assumes the ultrasound propagates in a straight line like x-rays, but which is false. Hence this assumption would be valid for soft tissue or in a smaller organ like breast, testicles, etc. where ultrasound travels without much diffraction and it can be measured in near field zone. When applied on a larger scale such assumption tends to fail, resulting in loss of minute tissue details and hence the image lacks resolution and reconstruction as stated becomes complex and expensive. Usually an ultrasound wave undergoes diffraction due to relatively large wavelengths associated with typical ultrasound sources forming a scattered field. The characteristic of the scattered field reveals the tissue property. This scattered field forms the base of the ultrasound computed tomography in diffraction mode. In our research we analyze that the ultrasound computed tomography in diffraction mode yields better resolution image in less computation time and in a strong scattering field.

The wave equation is theoretically and numerically solved considering the scattering term as a function of compressibility and velocity. The received field found by solving wave equation was simulated. The reconstruction of images for the measured data is very much essential in any system. These reconstructed images are a qualitative representation of the object of interest. Hence in our research USCT in diffraction mode

uses an alternate approach known as inverse scattering problem for reconstructing the parameters of interest. The reconstruction was carried out by using inverse non-uniform fast Fourier transforms with *l1*-norm. The reconstruction algorithm is written in Matlab code via fast Gaussian gridding. The convolution loops are written as C++ programs and are compiled as mex files from the Matlab command prompt. Initially a simple object of density 1020 kg/m^3 and with speed of sound 1540 m/sec was simulated Figure 27). This continuous medium is defined and is divided into evenly distributed mesh of grid points with pressure defined for each grid. A transducer is simulated and the input source is applied through transducer on the gridded medium. The sensor reads and calculates the scattered field. This can be reconstructed using reconstruction algorithms and output is displayed in amplitude spectrum. The reconstruction of this original data was performed using our proposed method and compared with the direct approach. The Figure 28.a. depict the reconstruction using direct method and Figure 28.b. represent the reconstruction using proposed method for 5 iterations both. It is seen that reconstruction using proposed method preserves more details and clearer.

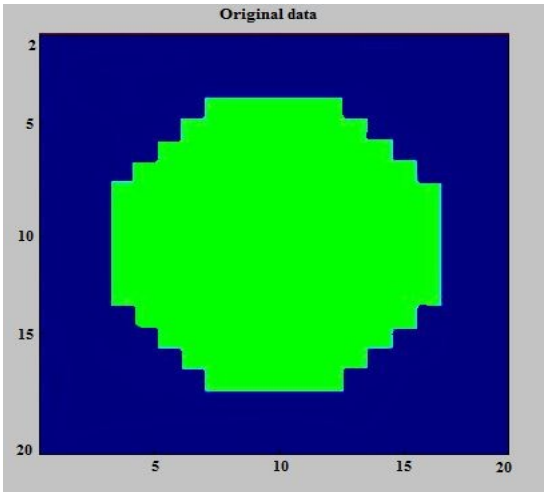

Figure 27: Original Data

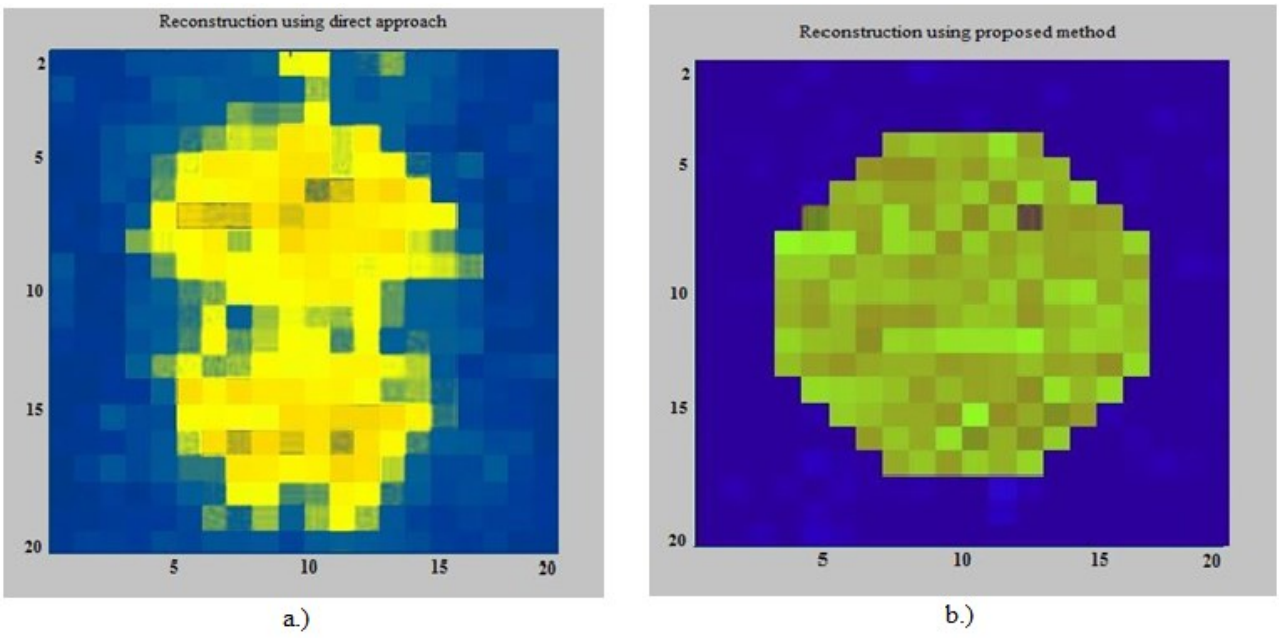

Figure 28: Reconstruction of Data Using a.) Direct Method and b.) Proposed Method

Next the Simulated data were performed on Shepp-Logan phantom which is much closer to reality and the medium was set using FOCUS software. This Shepp-Logan phantom is a superposition of ellipses representing features of the human brain with 64X64 pictures. The Fourier Transform of an ellipse is given by

$$E(K_x, K_y) = \rho e^{-i(K_x x^0 + K_y y^0)} \frac{AJ_1(B\sqrt{(u'AB^{-1})^2 + v'^2}}{\sqrt{(u'AB^{-1})^2 + v'^2}}$$

$$u' = K_x \cos\alpha + K_y \sin\alpha$$

$$v' = -K_x \sin\alpha + K_y \cos\alpha$$

(eq5.1)

A number of transducer ultrasound transmitters are positioned around the object in the ring configuration as in Figure 30. We simulated the number of transducer surrounding the object to be 76. The computation was performed on a basic system equipped by Intel Core i3 (2.1GHZ, 3Mb l3 Cache) and 750 GB HDD. The phantom is affected by

ultrasound plane wave and the scattering coefficient corresponding to the scattering field was reconstructed.

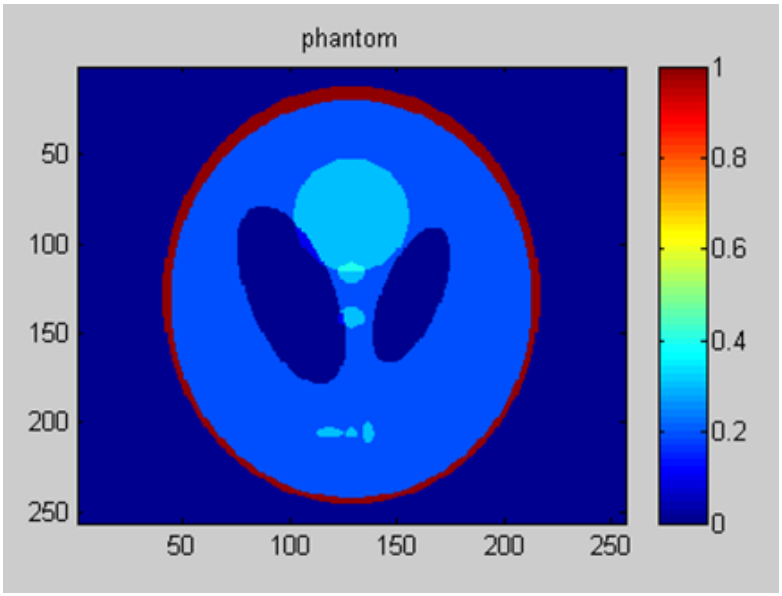

Figure 29: Original Data: Shepp-Logan Phantom

The scattering field is affected by 5% Gaussian noise. We tested the reconstruction of the phantom using basic inverse radon transform, Gridding algorithm and with non-uniform Fourier transform (NUFT). The same simulated data was next reconstructed using our proposed novel method.

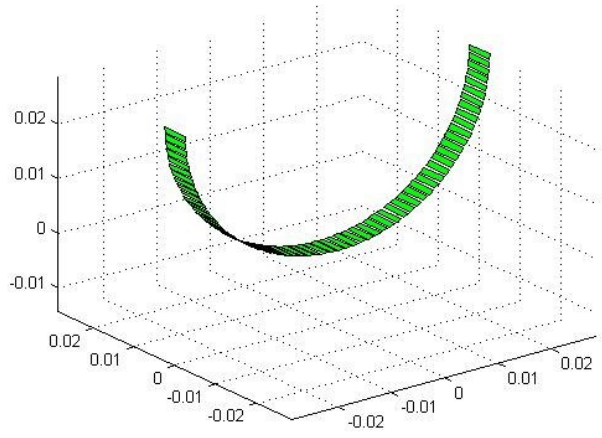

Figure 30: Placements of Ultrasound Transducers

Figure 29 shows the original image using Shepp-Logan phantom and compared with reconstruction using inverse radon transform and gridding algorithm depicted in Figure 31. The time taken for simulation using inverse radon transform with complexity $O(N^2)^3$ was approximately 79.07 seconds in comparison with gridding algorithm with complexity $O(4N^2+N^2Log(N^2)$ which took only 15.9 seconds.

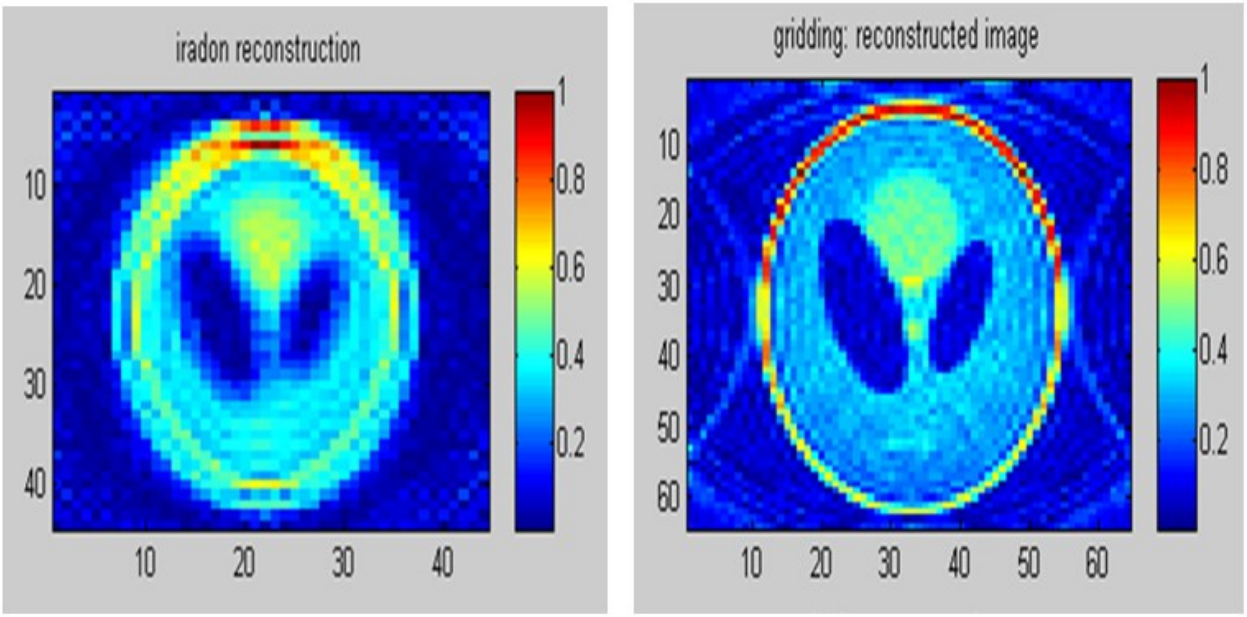

Figure 31: Reconstruction Using Inverse Radon (Left) and Gridding Algorithm (right)

Usually to reconstruct ultrasound non-uniform frequency samples, we consider non-uniform Fourier transform reconstruction approach such scattering term O(n) be the vector of the non-uniform distributed scattering term and F_n be the sample of a signal. Then Non-uniform Fourier transform can be implemented as

$$F_n=\sum f_{n\, e^{(-in\, O(n))}} \qquad \textit{(eq5.2)}$$

The dominant task in NUFT was calculation of iterative Fourier transform; therefore we propose a novel approach for reconstructing by modifying the NUFT for better computational time by using non-uniform fast Fourier transform with introduction of additional regularization term to prevent from over fitting. Figure 32 represents the reconstruction of simulated Shepp-Logan phantom using proposed method. The simulation algorithm used is described in brief below;

Simulation Algorithm

Initialize: O=0 and P=p_i

Condition: for n<N_{max}

Iteration:

- Compute P corresponds to O_n using *eq.4.36 and 4.38*
- Compute Regularization term corresponds to O_n
- Calculate a new value of O_{n+1} using *eq4.39*
- N=n+ 1**End**

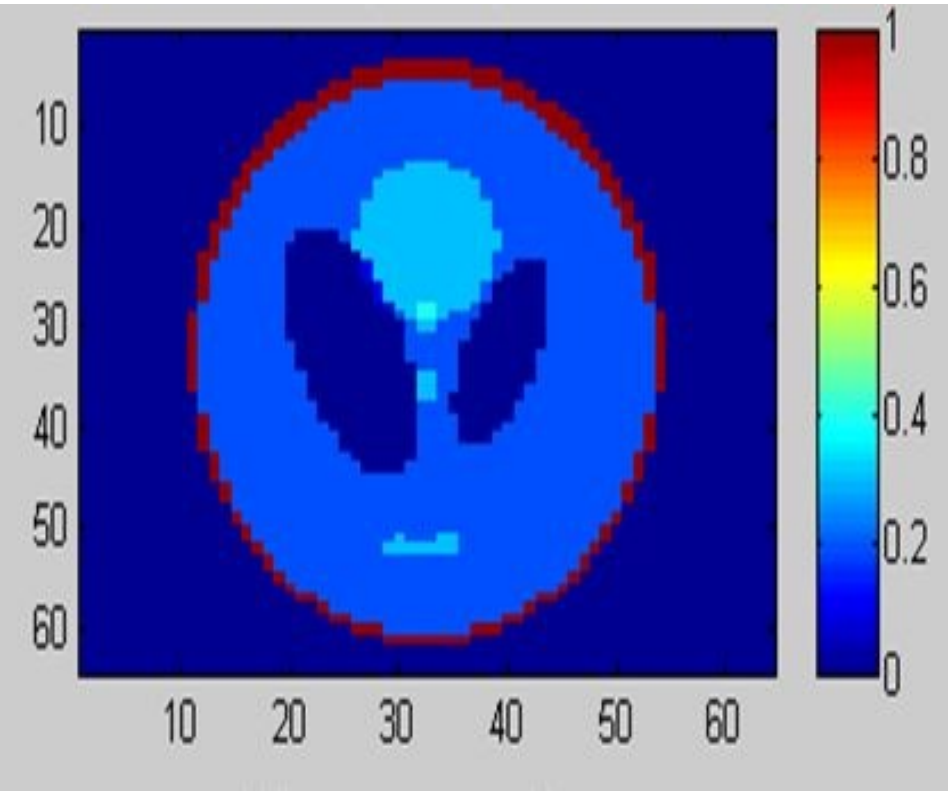

Figure 32: Reconstruction using proposed method

Reconstruction using proposed method with complexity $O(mNlogmN+mNlog(1/\varepsilon^2)$ produced immediate results in 7.85 seconds which is a faster process time for simulation. It clearly indicates that the proposed method highly restores the resolution of the image, when compared to other methods in Figure 31.

Table 5.1- Comparisons of Proposed Method with Various Other Reconstruction Methods

Reconstruction Procedure	Complexity	Time (sec)
Inverse Radon Transform	$O(N^2)^3$	79.07
Gridding Algorithm	$O(4N^2+N^2Log(N^2)$	15.9
Proposed Method	$O(mNlogmN+mNlog(1/\varepsilon^2)$	7.85

. The simulated data is a true match with our expected data. The Table 5.1 shows the comparisons of proposed method with Inverse Radon Transforms and Gridding

algorithm. The table clearly indicates that the proposed method decreases the time taking for the reconstruction. A computer simulation results with less than 10 sec is a better computational time while producing good resolution. The results indicate that the diffraction mode tomography using proposed reconstruction method yields high resolution image with decreased complexity.

6 Chapter: Conclusion and Future Work

Ultrasound imaging is a low-cost and non-invasive imaging modality; therefore it encourages to potentially advancing progression driven in low-cost and non-invasive diagnostic procedure. When working with a real tomography, to obtain a high resolution of the image reconstructed is quite complex and time consuming. An additional problem is how to compensate for involuntary motions of the patient during tomographic examination. Ultrasound computed tomography (USCT) is an emerging technology which aims at fast, safe and high resolution imaging. This technological attempt does not aim at replacing the computed tomography scanner or Magnetic resonance imaging system completely. This approach stands out with its own advantages. The major advantage of USCT is it is radiation free and does not involve any X-rays. The operational time is not long too. Usually a USCT can be developed as an automated system and hence reduces the operator dependent artefacts.

Ultrasound computed tomography research gained pace rapidly during 1970's and 1980's. But due to lack of advancements in the technology and software limitations it was not practically implemented. As the computation complexities ease decreased with novel methodologies and implementation, researchers have found new and easy ways of implementation. Currently, USCT for breast imaging is ready for clinical trials [48]. This approach is based on transmission and reflection mode tomography. Majority of application of USCT was devoted for imaging of soft tissue like detecting breast cancer, diagnosis of testicular cancer, etc. Many researchers have extended its applications in areas like diagnosis of hip dysplasia in newborns and search for inclusion and defects in bulk materials, brain but it lacked resolution. The possible reason is USCT assumes the

propagation of ultrasound in body tissues to be in straight line and apply the straight ray tomography approach and its reconstruction methods. In our research we have examined that the ultrasound does travel in 'some-what' straight line in soft tissues or in homogeneous medium. Also the transmission in smaller organs requires less time and hence the attenuation factor decreases. But when considering ultrasound propagation in other body organs or larger areas, the straight ray tomography approach fails i.e. it lacks resolution because the ultrasound waves diffracts due to the scattering terms. Hence the ultrasound that is diffracted has minute tissue details and should be taken into account while imaging along with reflection and transmission mode. This thesis was completely based on USCT in diffraction mode. Hence we solved the wave equation to estimate the tissue-sound interaction and propagation. Reconstruction of the image from the formulated equation can be very time consuming because it has no proper converging point. This ill posed problem can be solved into well posed by introducing of a regularization term. Regularization is a process of introducing additional information in order to solve an ill-posed problem or to prevent over fitting. One such is the Tikhonov regularization which most popular approaches to solve discrete ill-posed problems. But its applicability on ultrasound diffraction problem was tested using a computer simulation where the scattering term can be estimated using Tikhonov regularization with l1 regularization norm. The results indicate that the reconstruction with the proposed yielded image with higher resolution and with better computation time.

Simulation results indicate that derived method can yield images with higher image resolution in a strong scattering field in better computational time. Using Tikhonov regularization, the computation iteration was decreased and can greatly enhance the quality of reconstruction. As the computation complexities ease decreased with computing scattering term using Tikhonov regularization, we have a scope for new and easy ways of implementation. Our future work includes testing the accuracy and performance with other methodologies. As the sound needs a medium to travel, this ultrasound needs a coupling medium such as water or gel to transmit the ultrasound into the human body. So this coupling medium restricts the use of ultrasound to a smaller region because the entire body cannot be immersed into water or gel for imaging, and this seems to be impractical too. Henceforth Ultrasound computer tomography is more devoted to the diagnosis of benign and malignant tumors in soft and small biological tissues.

The future works encourages applying Ultrasound computed tomography for larger areas with the noticeable advancements in terms of software and hardware. Reducing the distance between body and transducer is a challenging task and essential too as the spatial and temporal resolution depends on frequency and distance between ultrasound transducers and area of interest. Our next future work also involves implementing this system as a wearable or attachable flexible wear-on dress with micro ultrasound transducers embedded on it such that these transducers would be in direct contact with the body during the scanning procedure and can be detached later. Therefore such system eliminates the use of immersing body in coupling gel or medium and

encourage for scanning of any area of body. This would also reduce the attenuation and the system would be portable and well as economical.

Also, USCT mostly uses an array of transducers and as the number of transducers increases the cost of equipment increases making USCT system no longer economical. Customarily ideal number of transducers used for a ring shaped arrangement can be 36 that have a beam, divergence angle of 70 degrees [16]. A better reconstruction quality is the achieved by widening the beam angle of the ultrasound transducer without expanding the number of transducers too. Therefore, lot of research the progressing toward these drawbacks and trying to implement an ideal standard practical Ultrasound computer tomography. Also, there is always room for software development such as it has huge scope for future advancements in 3D ultrasound diffraction computed tomography.

7 Chapter: Author Related Publications

1. Tejaswi, T. & Chris,J. (2014), Ultrasound Computed tomography in diffraction mode, The Journal of MacroTrends in Technology and Innovation, JMTI Vol 2 Issue 1 2014, ISSN 2333-1011 ISSN Online 2333-102x

2. Tejaswi,T & Chris,J. (2014), Regularization in Ultrasound diffraction tomography, Conference Proceedings of the Global Academic Network, GAN Journal. (To be published by late 2014)

References

1. Lindgren, Nilo, "Ultrasonics in medicine," Spectrum, IEEE , vol.6, no.11, pp.48,57, Nov. 1969 doi: 10.1109/MSPEC.1969.5214170
2. Dussik, K. T., Dussik, F. and Wyt, L.: Auf dem Wege zur Hyperphonographie des Gehirnes. Wien Med Wschr 97: 425, 1947
3. K. T. Dussik, Possibility of using mechanical high frequency vibrations as a diagnostic aid, Z. Neurol. Psychiat., vol. 174, pp.153 -168 1942
4. Firestone, F. A., U.S. Patent 2 280 226, granted April 1, 1942.
5. J.F.Greenleaf, S.A. Johnson, S.L.Lee,G.T.Hertman, and E.H.Wood. Algebraic reconstruction of spatial distributions of acoustic absorption within tissue from their two-dimensional acoustic projections, Acoustic Holography, 5:591-603, 1974
6. Mariappan, Leo, and Bin He, Magnetoacoustic Tomography with Magnetic Induction: Bioimepedance Reconstruction through Vector Source Imaging, March 2013
7. Golemati, S.; Gastounioti, A.; Nikita, K.S , Toward Novel Noninvasive and Low-Cost Markers for Predicting Strokes in Asymptomatic Carotid Atherosclerosis: The Role of Ultrasound Image Analysis, March 2013
8. Song, P., Zhao, H., Manduca, A., Urban, M. W., Greenleaf, J. F., & Chen, S. (2012). Comb-push ultrasound shears elastography (CUSE): a novel method for two-dimensional shear elasticity imaging of soft tissues. Medical Imaging, IEEE Transactions on, 31(9), 1821-1832.
9. Mace, E.; Montaldo, G.; Osmanski, B.; Cohen, I.; Fink, M.; Tanter, M., "Functional ultrasound imaging of the brain: theory and basic principles," Ultrasonics, Ferroelectrics and Frequency Control, IEEE Transactions on , vol.60, no.3, pp.492,506, March 2013
10. Ermilov, S. A., Conjusteau, A., Hernandez, T., Su, R., Nadvoretskiy, V., Tsyboulski, D.,& Oraevsky, A. A. (2013, March). 3D laser optoacoustic ultrasonic imaging system for preclinical research. In SPIE BiOS (pp. 85810N-85810N). International Society for Optics and Photonics.
11. Zografos, G., Koulocheri, D., Liakou, P., Sofras, M., Hadjiagapis, S., Orme, M., & Marmarelis, V. (2013). Novel technology of multimodal ultrasound tomography detects breast lesions. European radiology, 23(3), 673-683.
12. Marmarelis VZ, Kim TS, Shehada REN (2003) High resolution ultrasonic transmission tomography. Proc SPIE Med Imaging 5035:33–40

13. Jeong JW, Kim TS, Do SH, Shin DC, Singh M, Marmarelis VZ (2005) Soft tissue differentiation using multi-band signatures of high resolution ultrasonic transmission tomography. IEEE Trans,Med Imaging 24:399–408

14. Marmarelis VZ, Jeong J, Shin DC, Do SH (2007) High-resolution 3-D imaging and tissue differentiation with ultrasonic transmission tomography. In: Andre MP (ed) Acoustical imaging, vol 28,Springer, Dordrecht, pp 195–206

15. Tan Tran-Duc, Nguyen Linh-Trung, Michael L. Oelze, and Minh N. D, "Application of I1 Regularization for High-Quality Reconstruction of Ultrasound Tomography", 4th International Conference on Biomedical Engineering in Vietnam,, 2013

16. Yang, M., Schlaberg, H. I., Hoyle, B. S., Beck, M. S., & Lenn, C. (1999). Real-time ultrasound process tomography for two-phase flow imaging using a reduced number of transducers. Ultrasonics, Ferroelectrics and Frequency Control, IEEE Transactions on, 46(3), 492-501.

17. R Stotzka, J Wuerfel, Medical imaging by ultrasound computer tomography, TO Mueller, Medical Imaging, 2002

18. Haim Azhari (2010), Basics of Biomedical ultrasound for Engineers, John wiley & sons,Inc., Hoboken, New jersey.

19. Hem G T, 1980 Image Reconsmction from Pmjections: The Fmdamenrals of Compurerized Tomography(New York Academic)

20. Devaney A 1 1982 A filtered backpropagafion algoriltm for diffraction tomography Ulrrrosonic Imaging 4 pg 336-50

21. Kak A C and Slaney M (1987) Principles of Computerized Tomographic Imaging (New York IEEE)

22. Stenger F and O'Reilly M, Sinc inversion of the Helmholtz equation without computing the forward solution Preprint Department of Computer Science, University of Utah, 1994

23. F Natterer and F Wubbeling,A propagation-backpropagation method for ultrasound tomography, Inverse Problems,vol 11 1225, 1995.

24. Ulrich, W. D. (1971). *Ultrasound Dosage for Experimental Use on Human Beings*. NAVAL MEDICAL RESEARCH INST BETHESDA MD.

25. Greenleaf, J. F., Johnson, S. A., Lee, S. L., Wood, E. H., & Herman, G. T. (1974). Algebraic reconstruction of spatial distributions of acoustic absorption within tissue from their two-dimensional acoustic projections.

26. Greenleaf, J. F., Gisvold, J. J., & Bahn, R. C. (1982). Computed transmission ultrasound tomography. *Medical progress through technology*, *9*(2-3), 165.

27. Carson, P. L., Oughton, T. V., Hendee, W. R., & Ahuja, A. S. (1977). Imaging soft tissue through bone with ultrasound transmission tomography by reconstruction. *Medical physics*, *4*, 302.

28. Schreiman, J. S., Gisvold, J. J., Greenleaf, J. F., & Bahn, R. C. (1984). Ultrasound transmission computed tomography of the breast. *Radiology*, *150*(2), 523-530.

29. Johnson, S. A., Greenleaf, J. F., Tanaka, M., Rajagopalan, B., & Bahn, R. C. (1977). Reflection and Transmission Techniques for High Resolution, Quantitative Synthesis of Ultrasound Parameter Images. In *Ultrasonics Symposium, 1977* (pp. 983-988). IEEE.

30. Norton, S. J., & Linzer, M. (1979). Ultrasonic reflectivity tomography: reconstruction with circular transducer arrays. *Ultrasonic Imaging*, *1*(2), 154-184.

31. Kim, J. H., Park, S. B., & Johnson, S. A. (1984). Tomographic imaging of ultrasonic reflectivity with correction for acoustic speed variations. *Ultrasonic imaging*, *6*(3), 304-312.

32. Dines, K. A., & Goss, S. A. (1987). Computed ultrasonic reflection tomography. IEEE Transactions on Ultrasonics Ferroelectrics and Frequency Control, 34, 309-318.

33. Iwata, K., & Nagata, R. (1975). Calculation of refractive index distribution from interferograms using the Born and Rytov's approximation. *Japanese Journal of Applied Physics Supplement*, *14*, 379-384.

34. Stenger, F., & Johnson, S. A. (1979). Ultrasonic transmission tomography based on the inversion of the Helmholtz wave equation for plane and spherical wave insonification. *Appl. Math. Notes*, *4*, 102-127.

35. Mueller, R. K., Kaveh, M., & Iverson, R. D. (1980). A new approach to acoustic tomography using diffraction techniques. In *Acoustical imaging* (pp. 615-628). Springer US.

36. Devaney, A. J. (1982). A filtered backpropagation algorithm for diffraction tomography. *Ultrasonic imaging*, *4*(4), 336-350.

37. Devaney, A. J. (1983). A computer simulation study of diffraction tomography.*Biomedical Engineering, IEEE Transactions on*, (7), 377-386.

38. Pan, S., & Kak, A. (1983). A computational study of reconstruction algorithms for diffraction tomography: interpolation versus filtered-backpropagation.*Acoustics, Speech and Signal Processing, IEEE Transactions on*, *31*(5), 1262-1275.

39. WANG, H. Q., CAO, L. N., & CHAI, H. Z. (2013). Research on an Approach to Ultrasound Diffraction Tomography Based on Wave Theory.

40. Clement, G. T. (2013). Diffraction tomography on curved boundaries: A projection-based approach. *arXiv preprint arXiv:1312.6601*.

41. Gemmeke, H., & Ruiter, N. V. (2007). 3D ultrasound computer tomography for medical imaging. Nuclear Instruments and Methods in Physics Research Section A: Accelerators, Spectrometers, Detectors and Associated Equipment, 580(2), 1057-1065.

42. Ruiter, N. V., Zapf, M., Hopp, T., Dapp, R., Kretzek, E., Birk, M., ... & Gemmeke, H. (2012). 3D ultrasound computer tomography of the breast: A new era?. European Journal of Radiology, 81, S133-S134.

43. Osher, S., Burger, M., Goldfarb, D., Xu, J., & Yin, W. (2005). An iterative regularization method for total variation-based image restoration. *Multiscale Modeling & Simulation*, *4*(2), 460-489.

44. Hansen, P. C. (1987). The truncatedsvd as a method for regularization. *BIT Numerical Mathematics*, *27*(4), 534-553.

45. De Lathauwer, L., De Moor, B., & Vandewalle, J. (2000). A multilinear singular value decomposition. *SIAM journal on Matrix Analysis and Applications*, *21*(4), 1253-1278.

46. Ashfaq, M., & Ermert, H. (2004, August). A new approach towards ultrasonic transmission tomography with a standard ultrasound system. In Ultrasonics Symposium, 2004 IEEE (Vol. 3, pp. 1848-1851). IEEE.

47. ABUS-Shin, H. J., Kim, H. H., & Cha, J. H. (2011). Automated Breast Ultrasound. Journal of Korean Society of Ultrasound in Medicine, 30(3), 157-162.

48. Duric, N.; Littrup, P.; Roy, O.; Schmidt, S.; Cuiping Li; Bey-Knight, L.; Xiaoyang Chen, "Breast imaging with ultrasound tomography: Initial results with SoftVue," Ultrasonics Symposium (IUS), 2013 IEEE International , vol., no., pp.382,385, 21-25 July 2013 doi: 10.1109/ULTSYM.2013.0099

49. Neb Duric ; Peter Littrup ; Cuiping Li ; Olivier Roy ; Steven Schmidt ; Xiaoyang Cheng ; John Seamans ; Andrea Wallen ; Lisa Bey-Knight; Breast imaging with SoftVue: initial clinical evaluation, Proc. SPIE 9040, Medical Imaging 2014: Ultrasonic Imaging and Tomography, 90400V (March 20, 2014); doi:10.1117/12.2043768.

50. Bal, G., & Schotland, J. C. (2013). Ultrasound Modulated Bioluminescence Tomography. arXiv preprint arXiv:1310.7659.

51. Johns, L. D. (2002). Nonthermal effects of therapeutic ultrasound: the frequency resonance hypothesis. *Journal of athletic training*, *37*(3), 293.

52. Pan, S. X., & Kak, A. C. (1983). A computational study of reconstruction algorithms for diffraction tomography: Interpolation versus filtered-

backpropagation. *Acoustics, Speech and Signal Processing, IEEE Transactions on*, *31*(5), 1262-1275.

53. Chernov, L. A., & Silverman, R. A. (1967). Wave propagation in a random medium. New York: Dover publications..

54. Mettler, F. A., Huda, W., Yoshizumi, T. T., & Mahesh, M. (2008). Effective doses in radiology and diagnostic nuclear medicine: a catalog. Radiology, 248(1), 254.

55. Barrett, H. H., & Swindell, W. (Eds.). (1996). Radiological imaging: the theory of image formation, detection, and processing. Elsevier.

56. Brooks, R. A., & Di Chiro, G. (1975). Theory of Image Reconstruction in Computed Tomography 1. Radiology, 117(3), 561-572.

57. Gore, J. C., & Leeman, S. (1977). Ultrasonic backscattering from human tissue: a realistic model. Physics in medicine and biology, 22(2), 317.

58. Fatemi, M., & Kak, A. C. (1980). Ultrasonic B-scan imaging: Theory of image formation and a technique for restoration. Ultrasonic Imaging, 2(1), 1-47.

59. Jensen, J. A., & Svendsen, N. B. (1992). Calculation of pressure fields from arbitrarily shaped, apodized, and excited ultrasound transducers. Ultrasonics, Ferroelectrics and Frequency Control, IEEE Transactions on, 39(2), 262-267.

60. Morse, Philip M., and K. Ingard. "Uno: Theoretical Acoustics." (1968).

61. Jensen, J. A. (1991). A model for the propagation and scattering of ultrasound in tissue. Acoustical Society of America. Journal, 89(1), 182-190.

62. Firestone, F. A. (1949). U.S. Patent No. 2,483,821. Washington, DC: U.S. Patent and Trademark Office.

63. Canadian Institute for Health Information (CIHI), (2013, Feburuary 12). Medical Imaging in Canada 2012

64. Albany, NY (PRWEB). (2014, March 26). Global Medical Device Market to 2018. Retrieved April 1,2014